



Review

Secondary Zinc–Air Batteries: A View on Rechargeability Aspects

Sudheer Kumar Yadav Daniel Deckenbach and Jörg J. Schneider *

Fachbereich Chemie, Eduard-Zintl-Institut für Anorganische und Physikalische Chemie, Technische Universität Darmstadt, Alarich-Weiss-Strasse 12, 64287 Darmstadt, Germany

* Correspondence: joerg.schneider@tu-darmstadt.de; Tel.: +49-6151-162-1100

Abstract: Metal–air batteries hold a competitive energy density and are frequently recommended as a solution for low-cost, environmentally friendly electrochemical energy storage applications. Rechargeable zinc–air batteries are prominently studied future devices for energy storage applications. Up to date and despite substantial efforts over the last decades, it is not commercialized on a broader scale because of inadequate performance. Most essential, the ultimate long-term functional zinc–air battery has yet to be discovered. This challenge should be resolved appropriately before articulating the zinc–air batteries to commercial reality and be deployed widespread. We review the present status and some breakthroughs in rechargeable zinc–air batteries research in the last few years, focusing on the anode-related issues. A critical overview of the last five years of the still less explored but essential aspects of rechargeability in zinc–air batteries, such as zinc utilization, solid electrolyte interface, and cell design is presented, some perspectives on possible solutions are offered.

Keywords: zinc–air batteries; rechargeability; zinc anode; zinc utilization; solid electrolyte interphase; cell design



Citation: Yadav, S.K.; Deckenbach, D.; Schneider, J.J. Secondary Zinc–Air Batteries: A View on Rechargeability Aspects. *Batteries* **2022**, *8*, 244. <https://doi.org/10.3390/batteries8110244>

Academic Editor: Guanjie He

Received: 12 September 2022

Accepted: 15 November 2022

Published: 17 November 2022

Publisher's Note: MDPI stays neutral with regard to jurisdictional claims in published maps and institutional affiliations.



Copyright: © 2022 by the authors. Licensee MDPI, Basel, Switzerland. This article is an open access article distributed under the terms and conditions of the Creative Commons Attribution (CC BY) license (<https://creativecommons.org/licenses/by/4.0/>).

1. Introduction

At present, lithium-ion batteries are developing into the dominant energy source and storage medium. However, drawbacks, including scarcity of metal lithium stock, high prices, safety concerns, and less environmental friendliness, make them less practical for extensive energy storage applications. Metal–air batteries are studied as a capable substitute to lithium-ion technology, which can fulfill the ever-growing demand for low-cost, highly safe energy sources for electric automobiles or grid energy storage [1]. Metals including Li, Na, K, Zn, Al, Mg, Fe, Si, Ca, etc., are suitable for the usage as anode materials in metal–air batteries. The uniqueness of metal–air batteries represents the incorporation of gaseous oxygen from the surrounding atmosphere into the cell chemistry as an active cathode component, whose availability is inexhaustible due to the open-cell configuration. The unlimited supply of oxygen on the cathode side increases the energy density of the cell enormously and allows for long term cyclization by employing sufficient oxygen electrocatalysts without cathode active material deteriorating cyclic stability. Taking advantage of the unlimited oxygen supply, the commercially available primary zinc–air battery, which is possibly the best-known representative of the metal–air batteries so far, is pairing the oxygen-electrode with a zinc anode, which embodies hereby a highly desirable cell configuration with minimum amount of inactive material. Due to the inexhaustibility of oxygen on the cathode side, the zinc reservoir on the anode is the limiting factor regulating the energy taken from the cell. Thus, the complete oxidation of the zinc anode terminates the battery operation. Depending on rechargeability, metal–air batteries are broadly categorized in two categories primary and secondary (electrical rechargeable) batteries. Since the primary metal–air battery is designed for single-use operation the metal anode is sized to its largest preserving the battery operation for maximum duration, however this is never realized due to an incomplete utilization of the zinc reservoir caused by deactivation effects of the zinc metal anode (see below). In contrast to primary batteries,

electrically rechargeable metal–air batteries require the mutual adjustment of the anode and cathode to each other. While still having a continuous oxygen surplus at the gas diffusion electrode (cathode) the balancing of the metal anode becomes essential to ensure the rechargeable operation mode, where the metal reservoir should be optimized to achieve a complete and reversible transformation of the anode within every cycle. Constructing rechargeable metal–air batteries with an extended surplus of metal on the anode side, what can be understood as metal uninvolved in any electrochemical reaction during cyclization, fundamentally contradicts the guiding principle of electrical rechargeability and minimal usage of resources in such devices.

Breaking down rechargeability, probably the most important quality of a secondary battery compared to the primary equivalent is the operating life. Here, the metal–air battery poses special challenges for the development of rechargeable systems, since in addition to classic aging factors of battery materials, the influence of ambient air due to the semi-open cell system must also be taken into account. So far, the processes taking place at the gas diffusion electrode (cathode) are extensively characterized with respect to oxygen-electrocatalysis both in terms of material composition and electrochemical performance. Comprehensive studies focus on the longevity of the oxygen electrocatalysts while accepting non-application-oriented cell configurations considering the electrolyte volume, metal anode, and cyclization parameters, in order to obtain a sole and direct influence of the gas diffusion electrode on the rechargeability of the battery system. Thus, it would be highly desirable to adapt the cell system to realistic cycling conditions and to take a closer look at the interaction of the individual assemblies in the overall system. Here, the mass transfer of the full-cell system should experience a stronger focus, taking the battery operation under shortage of cell active materials into account. In rechargeable metal–air batteries, this material limitation is primarily to be found in the metal anode and the electrolyte but by definition not in the inexhaustible oxygen reservoir at the cathode side.

Among all the available metal–air batteries system, zinc–air batteries are encouraging because of their low-cost, competitive energy density, excellent security, and environmentally benign characteristics. This has led to the situation that primary zinc–air batteries were already commercialized early, however, commercial employments of secondary zinc–air batteries are scarce and are obstructed by low zinc utilization and inefficient plating/stripping performances on the anode side [2]. Plating and stripping refer to the processes of zinc deposition and dissolution on anode surface during cyclization. The metallic zinc anode undergoes complex chemical and electrochemical reactions during cyclization. When zinc is oxidized, soluble zinc species such as zinc hydroxides and zinate intermediates are generated. Upon super-saturation, the soluble species precipitate unevenly into non-conducting zinc species [3]. The non-conductive layer on the zinc anode metal surface increases the cell's internal electrical resistance and prevents further metal dissolution and, thus, zinc utilization. The nonconductive layer electronically isolates the active zinc surface in the discharge process, thereby typically ceasing discharge at ca. 50–60% zinc utilization. These phenomena also avert back deposition of zinc, effecting plating/stripping efficiency and restricting the rechargeability [4]. In a zinc–air battery system, the zinc anode is in immediate proximity to the electrolyte. The anode surface and interphase between anode and electrolyte are the primary reaction sites of rechargeable zinc–air batteries, and their quality determines the performance of the full battery cell [5]. To produce stable and rechargeable and durable zinc–air batteries, it is pivotal to understand and overcome the issues associated with the chemical activity, ion mobility, and mechanical feasibility of interfaces and interphases of the zinc anode. The still existing lack of a general agreement in defining a standard cell configuration to inspect the electrochemical properties at the laboratory scale exist one of the main hurdles in zinc–air battery investigations. The prevalent lab-scale cell configuration comprising abundant metal anodes, excess electrolyte, and carbon-based air electrodes can generate decent results. However, issues of lower zinc utilization and short cycle life still persist. Thus, the necessary improvement in the

cell configuration/design of rechargeable metal–air batteries is highly desirable for their commercial applications.

With respect to the cathode in ZABs a number of excellent reviews, concentrating on problems in developing these electrodes, e.g., studies towards the improvement or even displacement of carbon substrates and the advancement for efficient bifunctional catalysts have been reported [6–11]. On the contrary, very few reviews report issues of zinc anodes and the importance of electrolytes, solid electrolytes interface, and cell design in zinc anode and zinc–air batteries. The short lifetime for rechargeable zinc–air batteries is the major challenge. Herein, we believe that anodic malfunctioning is one of the main reasons for the shortfall in zinc–air batteries’ cyclability and lifespan. Deformation and demolition of the zinc anode are one of the main limitations of the performance of a zinc–air battery. In recent years, several research articles have reported high specific capacity comparable to theoretical capacity considering only consumed zinc mass instead of the total mass of zinc in the respective cells. This practice uses surplus zinc to maintain the supply during the losses in the side reactions occurring during charge and discharge.

The current review discusses concepts of zinc anode functioning and its optimization for maximum zinc utilization in zinc–air batteries. Electrolytes play a crucial role and govern the electrochemical reaction occurring in the vicinity of the electrodes. Optimization and modification of electrolytes, leading to enhancement in zinc anode and, ultimately, zinc–air battery performance, are also included. It also discusses the importance of developing solid electrolyte interphase (SEI) and acknowledgment of performance descriptors in following a standard cell design for zinc–air batteries. Primarily, operation of zinc–air batteries was reported at room temperature; however, an increase in human activities in different horizons has initiated the requirement for rechargeable batteries functional in different working conditions, a short discussion on zinc–air batteries with wide temperature adaptability is included. Thus, we review recent and important results on rechargeable zinc–air batteries, critically evaluate the justifications and offer potential future research directions (Figure 1). The discussion will be centered around the less explored but important aspects such as zinc utilization, solid electrolyte interface, and cell design in zinc–air batteries. The cathode side with its triple phase boundary between gas diffusion electrode, oxygen evolution reaction (OER) and oxygen reduction reaction (ORR) catalyst, and oxygen source is not part of this evaluation [7,12–15].

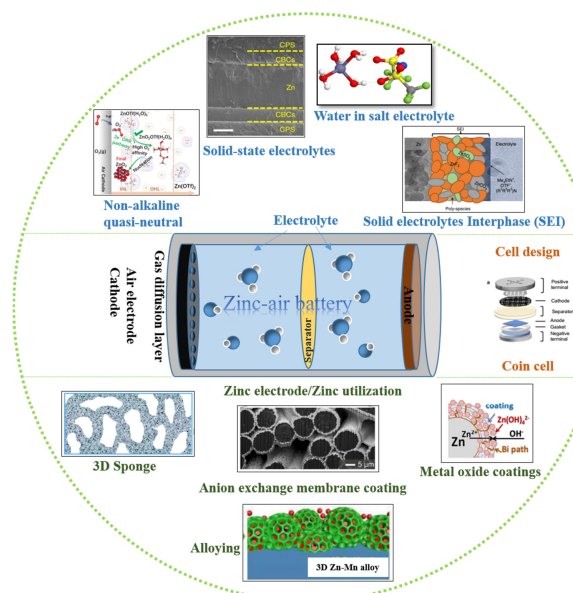
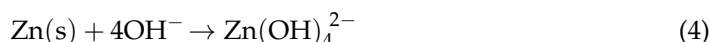


Figure 1. Overview of recent topical developments in zinc–air batteries covered.

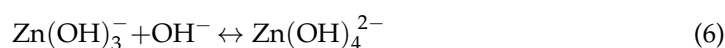
2. Anode Optimization as a Key to Zinc Utilization

Zinc utilization is described as the percentage of the theoretical capacity calculated with respect to the actual zinc mass used after the electrode is fully discharged. The problem with its correct determination is one of the principal causes of the variation in theoretical energy density versus practical energy density. Over the past two decades, compared to enormous research efforts on cathode electrocatalysts for zinc–air batteries, zinc anodes have received much less consideration than they deserve and what is indeed needed. Critical issues were mostly ignored in earlier research activities by using an excessive quantity of zinc metal due to its availability. However, as sustainability and closed materials cycles become ever more important this approach seems by far obsolete, a focus should be on minimization of such a resource as zinc. It is accountable that the depth of discharge (DoD) in the foregoing research is predominantly small (<10%) for rechargeable zinc–air batteries to exaggerate the effect of air cathodes. This low charging and discharging utilize only a very minor amount of zinc available rather than thriving to use fully what is available due to the surplus of zinc in the zinc metal anodes. In order to increase zinc utilization, maximum reversibility must be attained, which can be determined by the plating/stripping ratio and Coulombic efficiency (CE). In the coming ten years, the attainable aim would be to fabricate zinc anodes with practical material usage (>80%), cycle life (>500 cycles), high Coulombic efficiency (>80%), and the ability to discharge and charge (DoD > 50%) deeply. This aim has to be realized in technologically relevant zinc–air battery cells rather than experimental laboratory cells with excess electrolytes [16].

Zinc utilization and reversibility have to be viewed as unsatisfactory as long as the zinc electrode gets totally passivated or its inner defiance gets too elevated to keep a sustainable voltage [2]. In zinc–air batteries, a zinc metal anode in aqueous electrolytes is coupled with an air electrode with unlimited oxygen as a cathode reactant. The overall process in an aqueous electrolyte solution corresponds to the zinc being oxidized to Zn^{2+} releasing two electrons, which travel through the external circuit to the air electrode (Equations (1) and (2)), metallic zinc reacts with the hydroxide ions of the electrolyte to generate zinc hydroxide (Zn(OH)_2) and zincate (Zn(OH)_4^{2-}) (Equations (3) and (4)).



With the reaction continuously taking place, there is a rise in pH, and the electrolyte's pH significantly influences the reaction system. As described in the respective Pourbaix diagram (Figure 2) in highly alkaline solutions ($\text{pH} \geq 13$) Zn(OH)_4^{2-} is prevalent. On the other hand, when alkaline electrolytes have lower pH value (9.3 to 12.3), intermediary species like Zn(OH)_y^{2-y} were formed. Among this species, Zn(OH)_3^- and Zn(OH)_4^{2-} are reported to be dominant (Equations (4)–(6)). At lower pH, Zn(OH)_3^- is reported to be more predominant and is generated as a result of the OH^- depletion near to the electrode surface, which occurs due to a loss of displacement of (Zn(OH)_4^{2-}) ions [17,18].



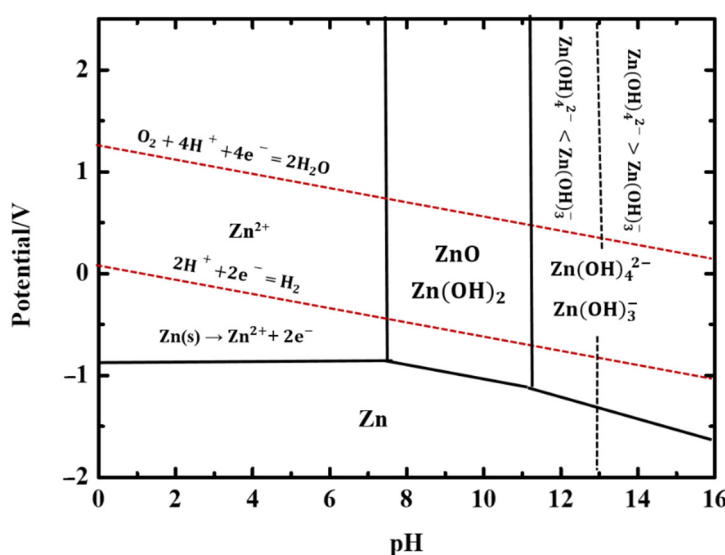
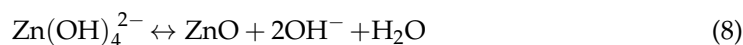


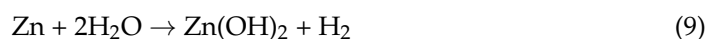
Figure 2. Pourbaix diagram of metallic zinc in water at different pH value. Reprinted with permission from Ref. [18], Copyright 2016, John Wiley and Sons.

With increasing pH, an apportion of zinc hydroxide and zinc would interact with hydroxide ions to form zincate which are finally dehydrated to form ZnO (Equations (7) and (8)) [18,19].



For zinc–air batteries two kinds of ZnO layers are discussed, viz. type I and type II [20–22]. For type I ZnO layer, formed by the dissolution–precipitation method, it is porous and limits OH^- ion diffusion to the exterior of the zinc anode; in consequence, hydroxide concentration drops consequently at the zinc anode/electrolyte interface [23]. The type II ZnO covering, formed during pH changes, is compact, irreversible, and passive. Using highly condensed alkaline solutions could decrease zinc passivation due to the dissolution of the passive layer. However, too high solubility will lead to shape and structural changes of zinc anode. Additionally, the development of the type II ZnO layer can be controlled moderately by managing the depth of discharge; however, it will decrease overall output energy. Passivation will not happen in the porous ZnO layers (type I) because of the necessary mass transfer of the hydroxide ions for anode reaction. The type II ZnO layer on repeated plating and stripping is supersaturated in the electrolyte and accumulated on the zinc anode, forming an insulating passivation film. A higher volume of ZnO in contrast to zinc metal is the reason for the harmful impact of the accumulated ZnO layers on the anode surface. Due to its hexagonal wurtzite structure, ZnO enlarge nearly 1.6 times the volume of the metallic zinc; thus, accumulation of ZnO film on the anode surfaces causes surface passivation and severe morphology changes [24]. In addition, the deposited ZnO film acts as a passivation layer because of its low electron mobility and large band gap (3.3 eV) at ambient temperature. On repeated plating/stripping, the deposited zinc oxide/zinc hydroxide layer thickens progressively as an insulating film on the entire zinc anode surface, which hinders further zinc dissolution. This loss of active zinc deteriorates the reversibility and is the major drawbacks in the growth of high-performance secondary zinc–air batteries [16]. During cyclization, the shape of zinc metal anodes steadily changes due to uneven plating and stripping, leading to an increase in roughness on the metal anode surface. The uneven plating and stripping may lead to dendrite formation. The dendrites formed on repeated plating/stripping will provoke battery short circuits/leakage and lead to weakened electrochemical activities, resulting in an irreversible zinc loss and, subsequently, short battery life [25]. In addition, the zinc anode also deteriorates from self-corrosion because of the hydrogen evolution reaction (HER) because zinc shows a

higher negative standard reduction potential compared to hydrogen, resulting in low zinc utilization. The HER reaction ingests zinc, producing zinc hydroxide and evolving hydrogen on the anode simultaneously (Equation (9)) [26]. Without suitable solutions to the aforementioned problems, the long-standing problem of a most effective cycling of rechargeable zinc–air batteries will not be achieved [27].



2.1. Zinc Electrode-Structural and Surface Optimization

In the following some recent significant developments in zinc anodes for secondary zinc–air batteries will be discussed. So far, two different approaches were followed to improve zinc utilization, zinc anode modification, and the optimization of the electrolyte composition. Generally, variation of the zinc anode-structures and their surface area enhancements are the strategies followed for zinc anode modification.

2.1.1. Structural Modification

The design criteria for zinc anode include requirements such as a stable structure to enable long-standing plating/stripping cycles of zinc ions free from collapse or profound shape change, substantial interspace for fast mass and ion transfer, a large surface area with active reaction spots to enhance exposure area across the zinc anode and electrolyte and finally support a uniform zinc deposition. Therefore, a variety of modifications to the zinc anode were explored, such as 3D sponges, fibers, foams, and particles [28]. For instance, the fabrication of zinc anodes with sponge-like 3D structures with monolithic void volume and interrelated zinc domains has been reported [3,29]. In contrast to standard zinc anodes, a newly developed 3D zinc anode architecture encourages consistent current diffusion and enhanced electron and ionic transport. The 3D structure can trap ZnO from the anodic process in its void space, decreasing the chances of metallic dendrite formation and enhancing discharge performance and increase in zinc utilization. The increase in zinc utilization in sponge 3D structured zinc anode is because of the presence of extended conductivity through the metallic zinc in the interior of the 3D sponge even if there is a zinc oxide coating on the sponge walls. In case of zinc powder as anode material particle to particle connectivity is lost resulting in high local current density and dendritic growth. In contrast, the 3D core-shell Zn@ZnO structure is persistent throughout the charge/discharge process, resulting in high zinc utilization and stable ZnO precipitation inside the void space, and reduced shape change upon cycling (Figure 3a) [29]. Sponge-like electrodes have also been reported in the fabrication of compressible and rechargeable solid-state zinc–air batteries, consisting of zinc sheets electrodeposited on nitrogen-doped carbon foams (NCFs) as zinc anode and Fe-doped Co₃O₄ nanowires on NCFs as the bi-functional air electrode (Figure 3b).

A zinc–air battery with a MOF-5 derived nanoscale 3D porous ZnO/C anode was recently introduced which allows for an enhanced zinc utilization [17]. The composite ZnO/C anode expresses a notable improvement in rechargeability, realizing 267 mAh/g of a discharge capacity with 32.6% DoD. (Figure 4c). The discharge capacity is stable over the 60 cycles for ZnO/C anode. In contrast, zinc foil (32 mAh/g, 4% DoD) and zinc powder (105 mAh/g, 12.8% DoD) anodes show sharp decay of discharge capacity after 27 and 21 cycles, respectively (Figure 4a,b). The improved rechargeability, cyclability and zinc utilization in case of the ZnO/C composite is due to its 3D porous structure. The ZnO/C anode does not show dendrite formation whereas zinc foil (Figure 4d) and zinc powder (Figure 4e) anodes show voluminous dendrite formation and electrode deterioration.

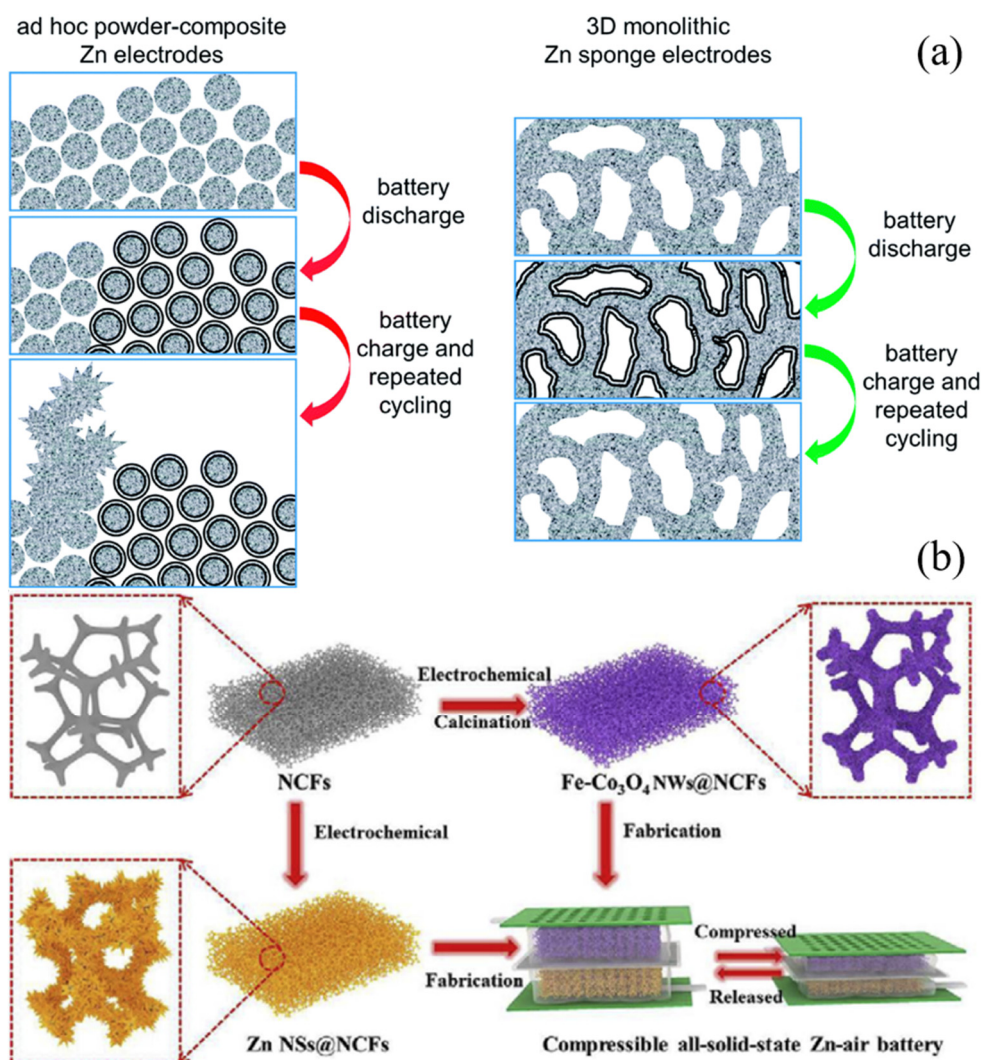


Figure 3. Graphic representation of (a) the zinc oxide dissolution and deposition traditional powder-composite zinc anode and the zinc wire (3D-sponge structured) anode [29], Reprinted with permission from Ref. [29], Copyright 2014, The Royal Society of Chemistry; and (b) fabrication method for the compressible and rechargeable solid-state zinc–air battery [28]. Reprinted with permission from Ref. [28], Copyright 2019, Elsevier.

To further improve cyclic stability, a 3D zinc anode modified with Ag nanoparticles was reported [26]. The anode was fabricated by coating a uniform layer of Ag nanoparticles on Cu foam framework followed by electrodeposition of zinc (Figure 5a). The Ag coating increases the HER overpotential, which leads to a reduction in self-corrosion of zinc anode. The highly conductive Ag nanoparticles furnish uniform and uninterrupted electron transfer channels through the 3D framework, which endow low overpotential deposition spots for zinc deposition (Figure 5b). This leads to guided uniform zinc deposition during the changing/discharging process and reduced zinc dendrite formation. The fabricated secondary zinc–air battery with Ag-improved 3D zinc anode exhibits a 94% of Coulombic efficiency after 80 cycles with 2 h each cycle duration (Figure 5c).

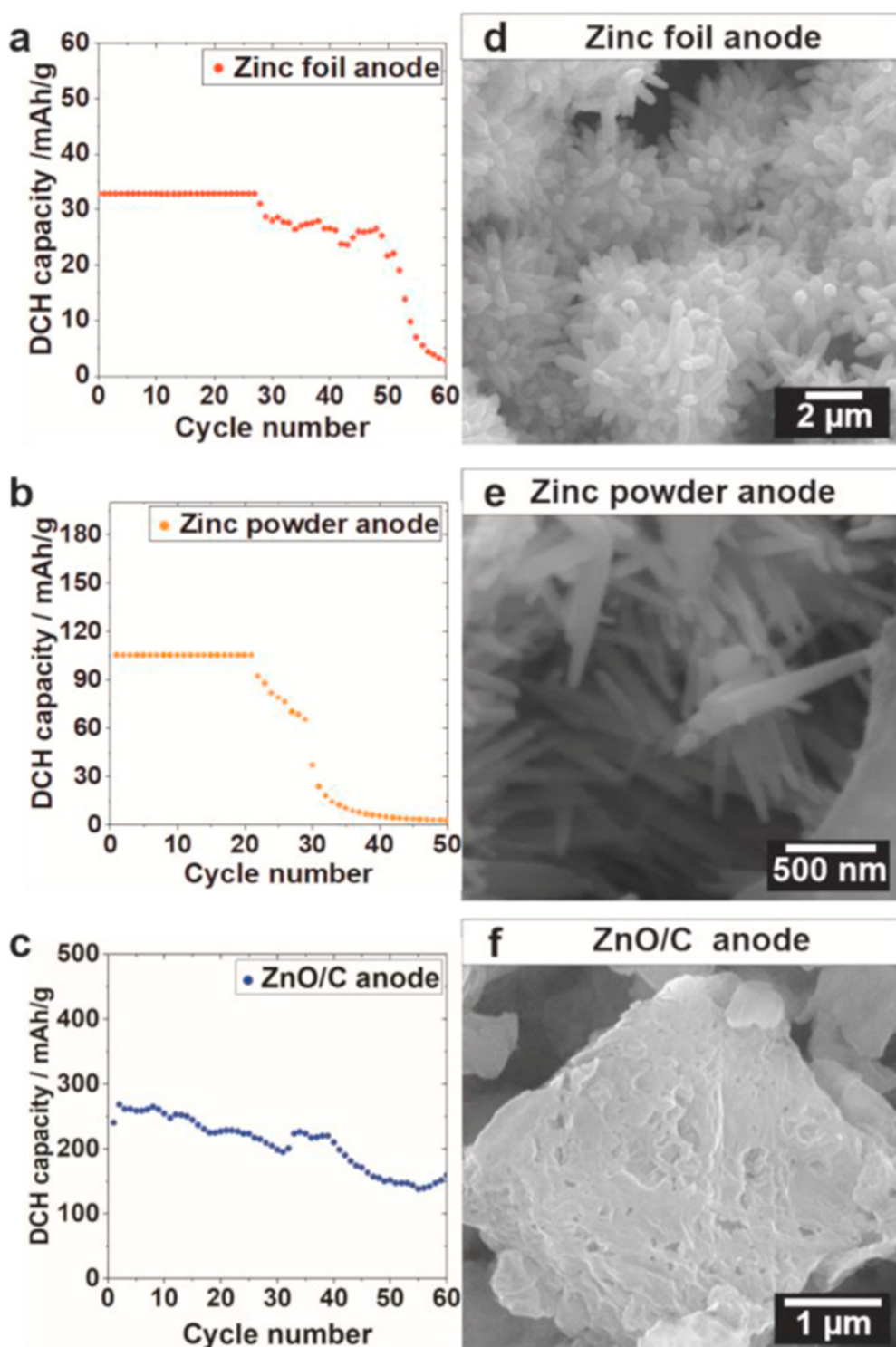


Figure 4. Galvanostatic cycling of zinc anode with different morphology; (a,b) the zinc foil anode displayed steady cycling (27 cycles) with 32 mAh/g of discharge capacity and zinc powder exhibits 105 mAh/g of discharge capacity for 21 cycles. (c) ZnO/C composite anode exhibits maximum discharge capacity of 267 mAh/g because of enhanced zinc availability. The SEM image of ZnO/C confirms no dendrite formation (f), whereas zinc foil and zinc powder anodes displayed voluminous dendrite generation and electrode destruction (d,e) [17]. Reprinted with permission from Ref. [17], Copyright 2021, Elsevier.

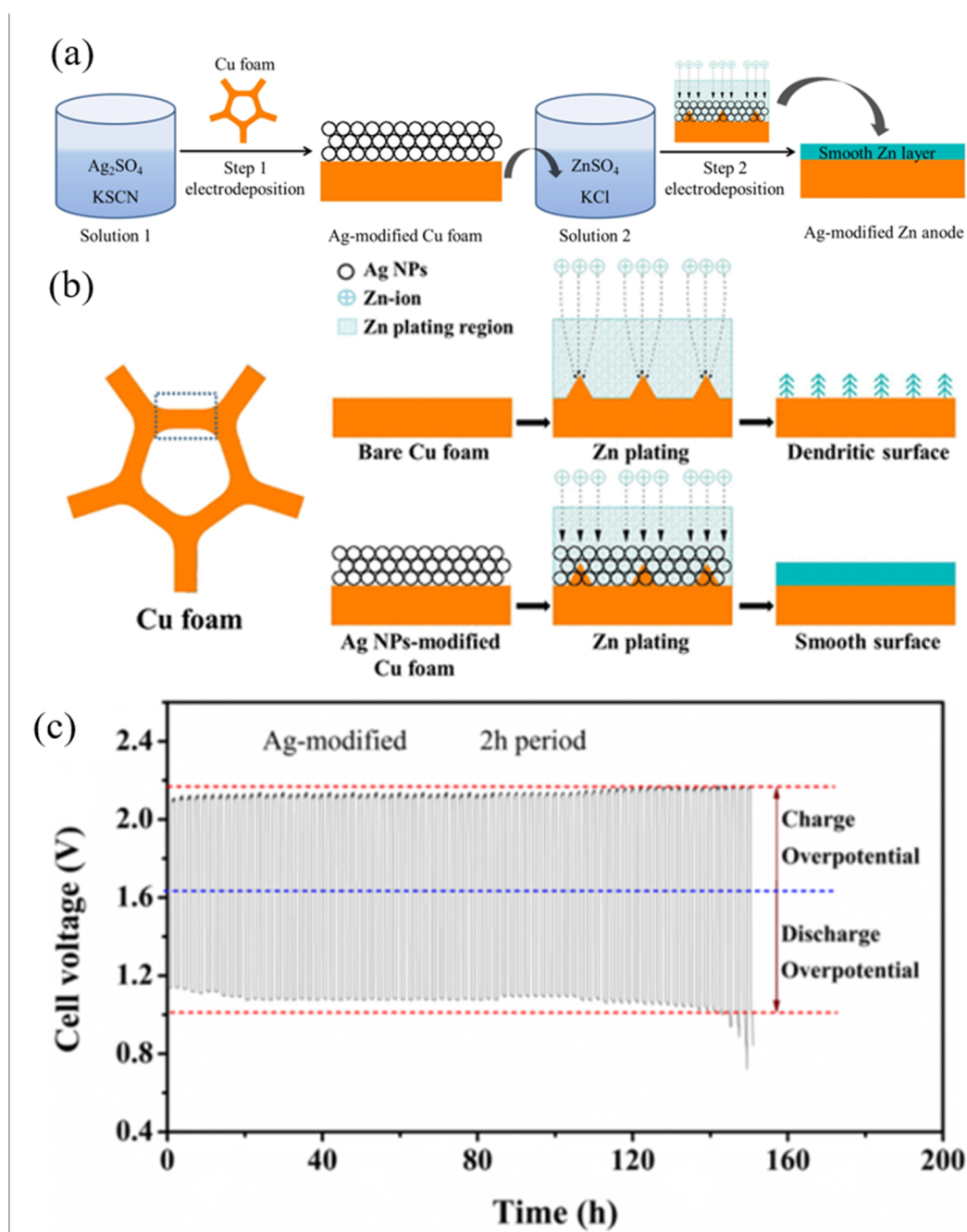


Figure 5. (a) Schematic representation of the construction method of Ag-modified 3D zinc anode, (b) schematic illustration of zinc deposition process on plain Cu foam and Ag-modified Cu foam and (c) the charge–discharge cyclic activity of zinc–air battery fabricated with Ag-modified zinc anode (2 h cyclic duration) [26]. Reprinted with permission from Ref. [26], Copyright 2019, American Chemical Society.

Structural optimization of the zinc anode by electrochemical methods is a recently introduced method to enhance rechargeability in zinc–air battery system. The electrochemical method produces highly pure and porous nanostructures. For example, fabrication of a porous zinc anode by electrochemical reduction of ZnO . The ZnO to Zn phase transition was carried out at a fixed potential (-1.6 V vs. saturated Ag/AgCl) in an electrolysis cell with a 3 M KOH electrolyte (Figure 6a) [30]. The zinc–air coin cell was built with nanoporous zinc as the anode, a minimal electrolyte (9 M KOH), and $\text{Pt/C}/\text{IrO}_2$ as the cathode (schematically shown in Figure 6b). The minimal electrolyte assures a small proportion of the electrolyte to the zinc anode capacity (0.03 mL/mAh), to be interpreted as an

actual zinc–air battery. Figure 6c shows cyclic performance at 10 mA/cm^2 of the fabricated zinc–air battery for a period of 80 h.

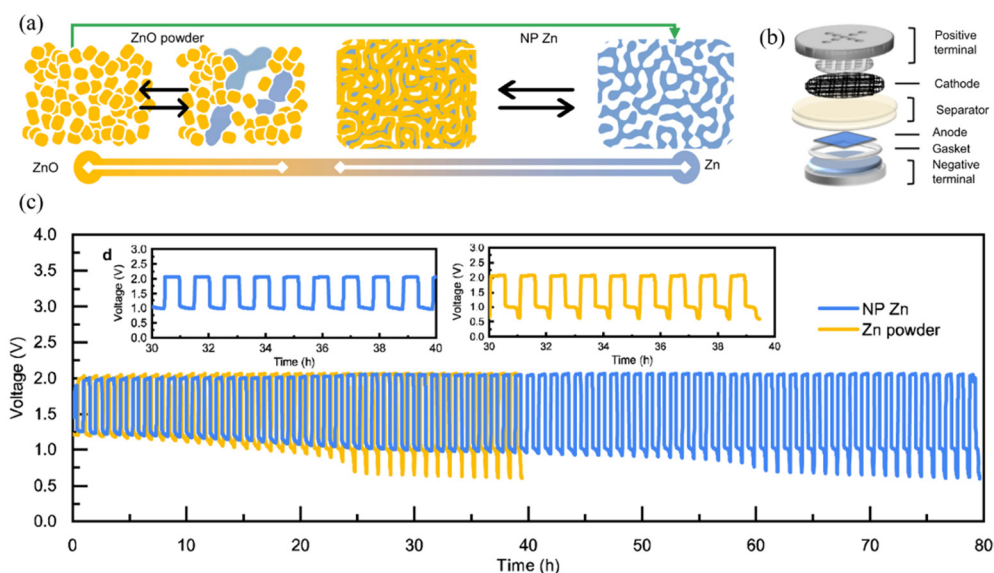


Figure 6. (a) Representation of the distinct pathways of transformation with unmixed ZnO (shown by yellow color) on the extreme left and unmixed zinc (shown by blue color) on the extreme right. The ZnO powder is the anode, and the transition is between powder and clusters of zinc metal (in the left-black arrows). Alternately, enhanced transition (shown by the green arrow) results in nanoporous zinc (in the right-black arrows), (b) schematic presentation of the zinc–air coin cell reported. and (c) potential vs. time curves at current density of 10 mA/cm^2 with 10% DoD. [30]. Reprinted with permission from Ref. [30], Copyright 2022, Springer Nature.

However, it is crucial to understand that a zinc anode with a high surface area leads to anode corrosion and parasitic hydrogen evolution due to enhanced contact between anode and electrolyte. This will lead to an enhanced self-discharge while the battery is non-functional and deteriorates the battery's Coulombic efficiency. Thus, research aiming towards further improved zinc anodes with extensive active surface area should focus on methods to mitigate corrosion and hydrogen evolution.

Another way to improve zinc anode efficiency is by fabricating alloyed anode materials, using Zn-M alloy as the prototype (M = transition metals). Recently, a 3D Zn_3Mn alloy anode fabricated by an electrodeposition method was reported [31]. The standard electrode potential of Mn^{2+}/Mn is notably lesser than Zn^{2+}/Zn , which creates an electrostatic shielding effect and impedes zinc dendrite creation during zinc deposition over Zn-M alloyed anode surface. Compared to zinc, the Zn_3Mn alloy anode has comparatively elevated binding energy on the surface, which assists in directing and governing zinc nucleation and growth and reduces the dendrite development at the beginning of zinc deposition. Further, the porous 3D nanostructure controls zinc ions' distribution kinetics, which reduces the dendrite generation for the whole zinc deposition duration (Figure 7a). Density functional theory (DFT) and experimental investigations demonstrated that the Zn_3Mn anode has superior interfacial durability, realized because of uniform Zn^{2+} distribution passage on the Zn_3Mn anode surface. The fabricated Zn_3Mn alloy displayed better power density, discharge capacity, and cycling performance over 6000 min without degradation at 10 mA/cm^2 than the zinc–air batteries fabricated with commercial zinc anodes (2760 min with a vast hysteresis behavior) (Figure 7b). The Zn_3Mn alloy is also mechanically durable and was used to fabricate flexible zinc–air batteries, and under repeated bending-twisting, the flexible zinc–air battery tandem cells demonstrate a stable voltage. Moreover, zinc-ion battery with Zn_3Mn alloy anode, MnO_2 cathodes and seawater-related electrolyte (0.1 M MnSO_4 and 2 M ZnSO_4 in seawater) also displayed stable charge/discharge performance

as compared to zinc-ion battery with zinc anode (Figure 7c). Another example is zinc-tin (Zn-Sn) alloy fabricated with a simple powder sintering method, and the alloy as an anode remarkably enhance the performance of a secondary zinc–air battery [32]. Compared to pure zinc foil, the ZnSn10 alloy displayed lower voltage hysteresis, higher power density and current density, and a long cycle lifespan (200 h) with stable voltage discharge curves. The theoretical simulation illustrates that the fabricated alloy structure controls the anode's charge diffusion and electron density and stimulates zinc stripping/plating reversibility with minimal dendrite formation. Meanwhile, the strong and surplus Zn-Sn interphase sustains the chemical stability to restrain the corrosion. Thus, the functional ZnSn10 alloy anode displayed excellent dendrite-free zinc stripping/plating performances with significantly small overpotential and superior corrosion resistance. Other material combinations to be alloyed with zinc are metals such as silver, copper, aluminum, bismuth, cadmium, and lead, and their oxides [26,33–37]. For instance, bismuth and its oxides are frequently reported because of their good thermal reliability and high electrical conductivity. They show however, a tendency to form a SEI on the zinc anode surface which assist to decrease extent of passivation and corrosion [34,37].

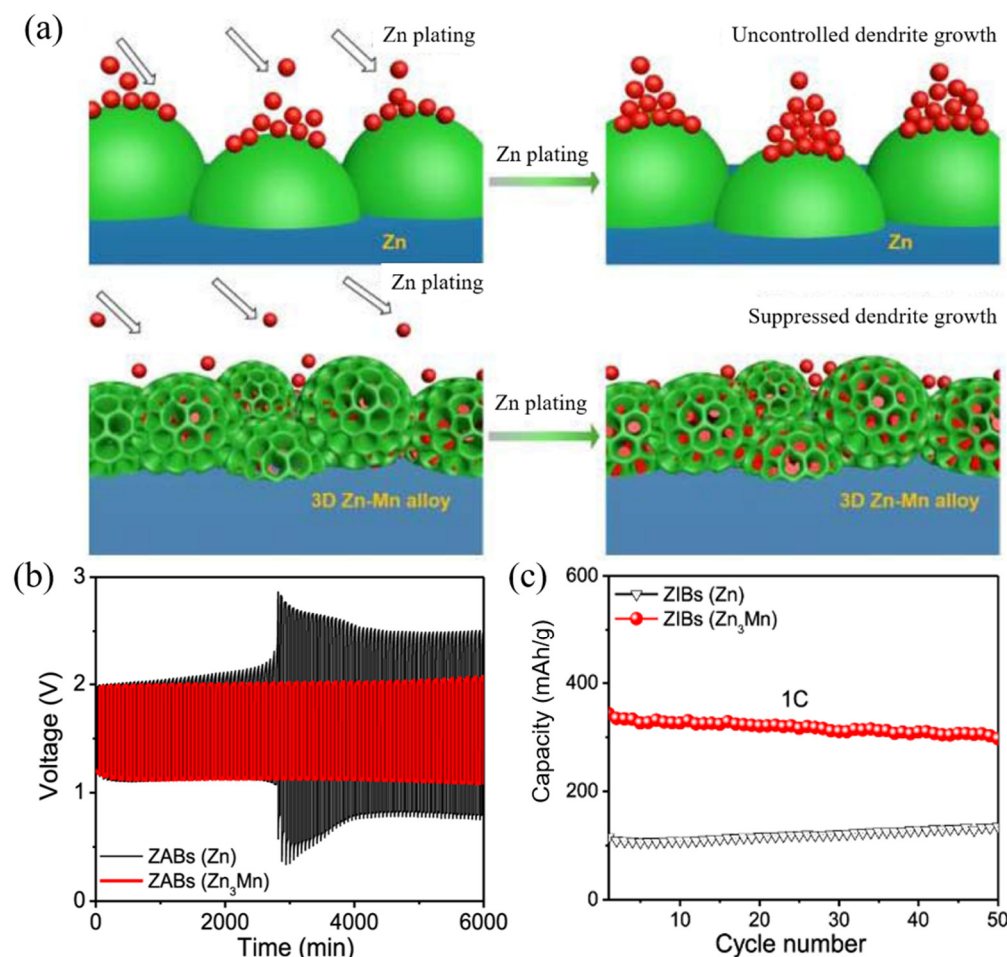


Figure 7. (a) Schematic representation of the zinc deposition process on pure zinc anode and Zn_3Mn alloy anode. (b) Cycling performance of zinc–air batteries with Zn_3Mn alloy and Zn anode. (c) Cycling performance of zinc-ion battery (Zn_3Mn and Zn) at 1C using seawater-based electrolyte [31]. Reprinted with permission from Ref. [31], Copyright 2021, Springer Nature.

The tendency to form nonplanar and non-uniform zinc electrodeposits while continuous stripping/plating is crucial reason for the short cycle life of secondary zinc–air batteries. However, if zinc deposits can be controlled at the surface on the microscopic level, the undesirable dendrite formation can be retarded or even completely obstructed

to assure superior reversibility. Development of anodes with a well-defined zinc–metal alloy composition are a definite asset to achieve a betterment in that realm. An *in situ* electrochemical zinc anode structural optimization has been reported using phosphoric acid (H_3PO_4) as an additive in zinc sulphate ($ZnSO_4$) electrolyte [38]. The addition of H_3PO_4 leads to texturing of zinc anode surface ([002]-textured) as well creation of a solid-electrolyte interphase layer (SEI). The zinc-metal anode textured with preferential zinc [002] deposition suppresses dendrites formation, shows corrosion resistance, and reduces the physical contact between the electrolyte and the electrode, inhibiting side reactions and improving the battery performance.

2.1.2. Surface Modification

Surface alteration of zinc anodes can also include coating with different ion-sieving nanoshells. Such surface coated nanoshells permit hydroxide ion passage and restrict zincate ion movement. The zincate ions are immobilized and react with zinc in the coated nanoshell, limiting non-uniform zinc deposition. The immobilized zinc is oxidized to ZnO , after reaction with freely movable hydroxide ions. Coating of zinc or ZnO anode with ion sieving oxides (e.g., graphene oxide, CuO , Al_2O_3 , SiO_2 , TiO_2 , TiN_xO_y) and carbon nanostructures have been recently reported [4,39–45]. For instance, TiO_2 acting as an ion sieving compound over zinc anode was fabricated by coating submicron sized ZnO nanorods with TiO_2 shell (HSSN) [44]. The TiO_2 layer acts as blocking layer for zincate ions, reducing passivation, dissolution and HER. As anticipated, the uncoated ZnO nanorods anode showed structural deformation after the charge/discharge cycles (Figure 8a). However, ZnO anode layered with TiO_2 shell was able to sustain its initial structure arrangement after charge/discharge cycles. The fabricated $ZnO@TiO_2$ anode displayed excellent reversible deep cycling performance under minimal electrolyte conditions (170 cycles, 40% DoD) (Figure 8b). Moreover, the cyclic performance at 100% DOD in the minimal electrolyte survived for 33 cycles with a Coulombic efficiency of 93.5%.

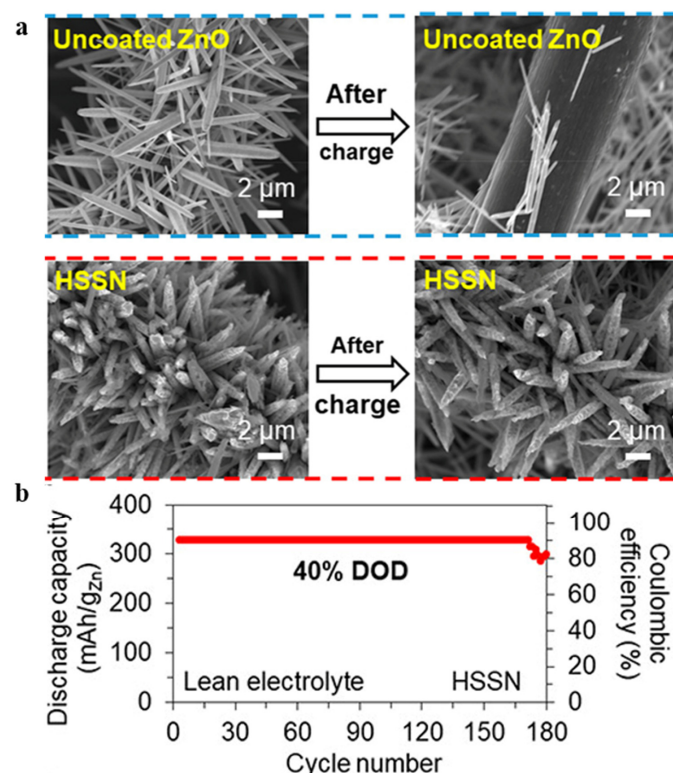


Figure 8. (a) SEM images for uncoated ZnO anode and the $ZnO@TiO_2$ (HSSN) anode before and after charging. (b) Cycling performance of the HSSN anode at 40% DOD in the minimal electrolyte [44]. Reprinted with permission from Ref. [44], Copyright 2020, American Chemical Society.

Another example of an ion-sieving coating is when ZnO nanoparticles are coated with carbon nanoshells (ZnO@C). The ZnO@C anode battery displayed 100 cycles activity with efficiency >90% and 100% DoD, considerably enhanced performance than the uncoated ZnO nanoparticles and zinc foil (Figure 9A [46]). Apparently, the uncoated ZnO anode surface shows depressions and deterioration after cycling, (Figure 9B,C, resulting from ZnO dissolution. In contrary, the ZnO@C anode sustain its structure and morphology after cycling (Figure 9D,E, which verifies the carbon shell's capability on ZnO@C to reduce zinc anode dissolution and passivation.

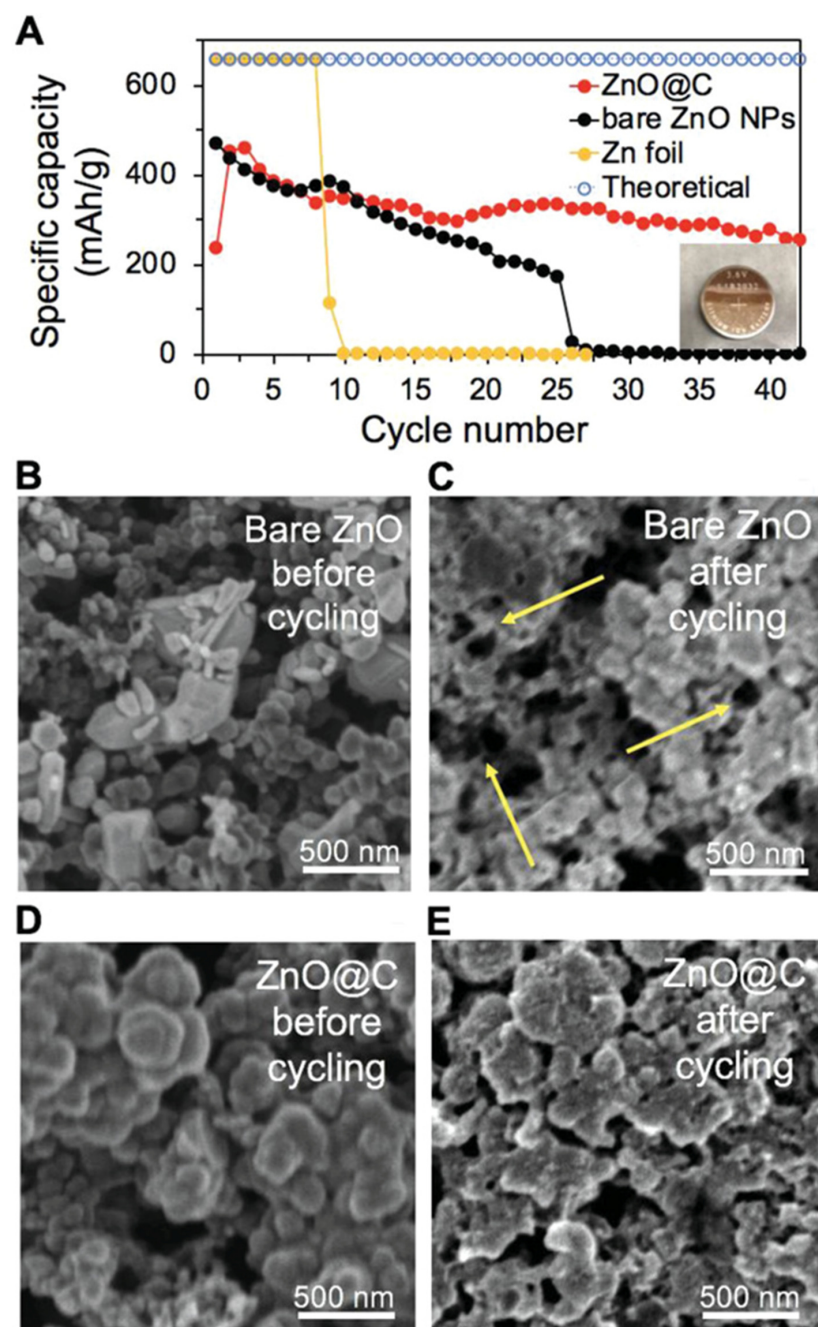


Figure 9. (A) Specific discharge capacity of uncoated ZnO, zinc foil and ZnO@C anodes over the discharge process. SEM micrograph of uncoated ZnO anode (B) before cycling, (C) after three cycles, holes are shown by yellow arrows. SEM micrograph of ZnO@C anode (D) before cycling and (E) after three cycles [46]. Reprinted with permission from Ref. [46], Copyright 2018, John Wiley and Sons.

The coating of glassy material may also enhance the current distribution and conductivity and boost a dense zinc deposition process which increases reversibility and rechargeability [47]. For instance, bismuth and calcium oxides were explored to modify the zinc anode by coating a layer of 3.2 wt% of Bi_2O_3 – ZnO – CaO glass composite. SEM micrograph of bare and coated zinc are displayed in Figure 10a,b, respectively. The coating forms a porous structure during cyclization, creating conductive pathways for Bi ions. This is verified by the decrease in internal resistance after cycling. In the case of coating of glass, internal resistance $\Delta R_i \cdot \text{AM}^{-1}$ was 4.39 Ω , which is lesser than without glass coating (6.54 Ω) (Figure 10c). Due to interaction amongst ZnO , Bi_2O_3 and CaO the cyclic stability of coated zinc electrode is strikingly improved to 20 cycles as compared to an uncoated one (Figure 10d). Moreover, there was an increase in initial zinc utilization up to 62% for a coated zinc anode as compared to 53% for a bare zinc anode. Thus, because of the creation of conductive Bi pathways and trapping of zincate ions inner side of the coating layer, the coating approach led to high zinc utilization and improved rechargeability [48].

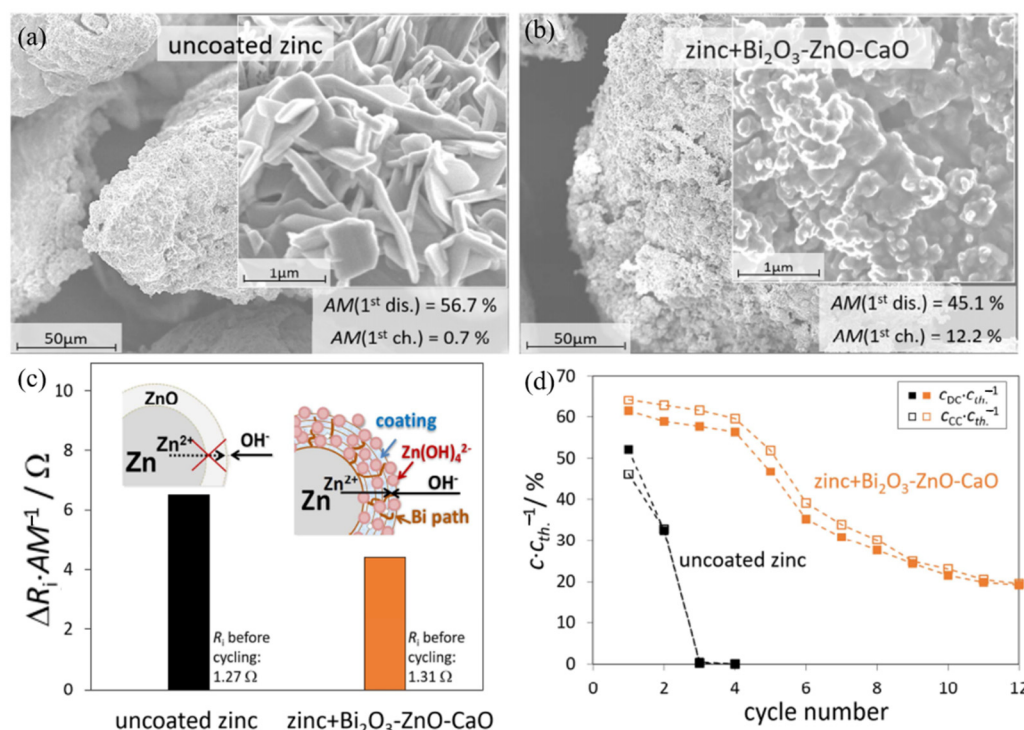


Figure 10. SEM micrograph of bare zinc (a) and coated zinc (b); (c) ohmic resistance ΔR_i , depends on active zinc utilization AM, of bare zinc and zinc covered with 3.2 wt.% Bi_2O_3 – ZnO – CaO , together with the graphic representation of passivation behavior of the zinc particles; and (d) cyclic performance of zinc–air batteries utilizing bare and coated zinc [48]. Reprinted with permission from Ref. [48], Copyright 2018, Elsevier.

Organic polymer coatings have benefits such as low cost, simple fabrication, and can be environmentally benign in contrast to inorganic anode coatings. Coatings such as polyvinyl alcohol (PVA), polyaniline (PANI), and sodium polyacrylate (PANa) hydrogel on zinc anode were explored for upgrading self-discharge and anti-corrosion [49,50]. For instance, in the composite ZnO /PVA/β-CD/PEG, the polymer binders help to create a firm porous 3D framework electrode, which confines the zinc metal and diminishes anode deformation leading to dendrite-free 80 cycles [51]. Another example is fabrication of novel PANI/Zinc-phthalocyanine nanocomposite (PANI@ZnPc) as zinc electrode [50]. The fabricated zinc–air battery with coated zinc anodes shows stable cyclic performance (120 h). Recently introduced ionomeric polymer coatings anion-exchange ionomer (AEI) or ionomeric hydroxide-conducting polymer (IHCP) over the zinc anode are reported to enhance zinc utilization [52–54]. For instance, a novel approach was followed to fabricate

zinc anodes comprising carbon mesh as host material. Onto this a uniform layer of zinc oxide was deposited and subsequently coated with IHCP (Figure 11a) [53]. The IHCP coating acts as hydroxide conducting layer and confine zincate ion inhibiting its loss in bulk electrolyte. Carbon mesh act as electronic conductive high surface area host framework and the active substance was ZnO instead of zinc to evade further volume expansion on cycling. Figure 11b,c represent cycling performance of Zinc–O₂ battery fabricated with IHCP (here fumion®–FAA3 (Fumatech)) coated ZnO anode and a ,gas diffusion electrode with a Sr₂CoO₃Cl catalyst. It exhibits 13 cycles (charge/discharge) with average Coulombic efficiency of 71.1% and specific capacity (Q_{dis}) of 351 mAh/g (DoD of 53.6%).

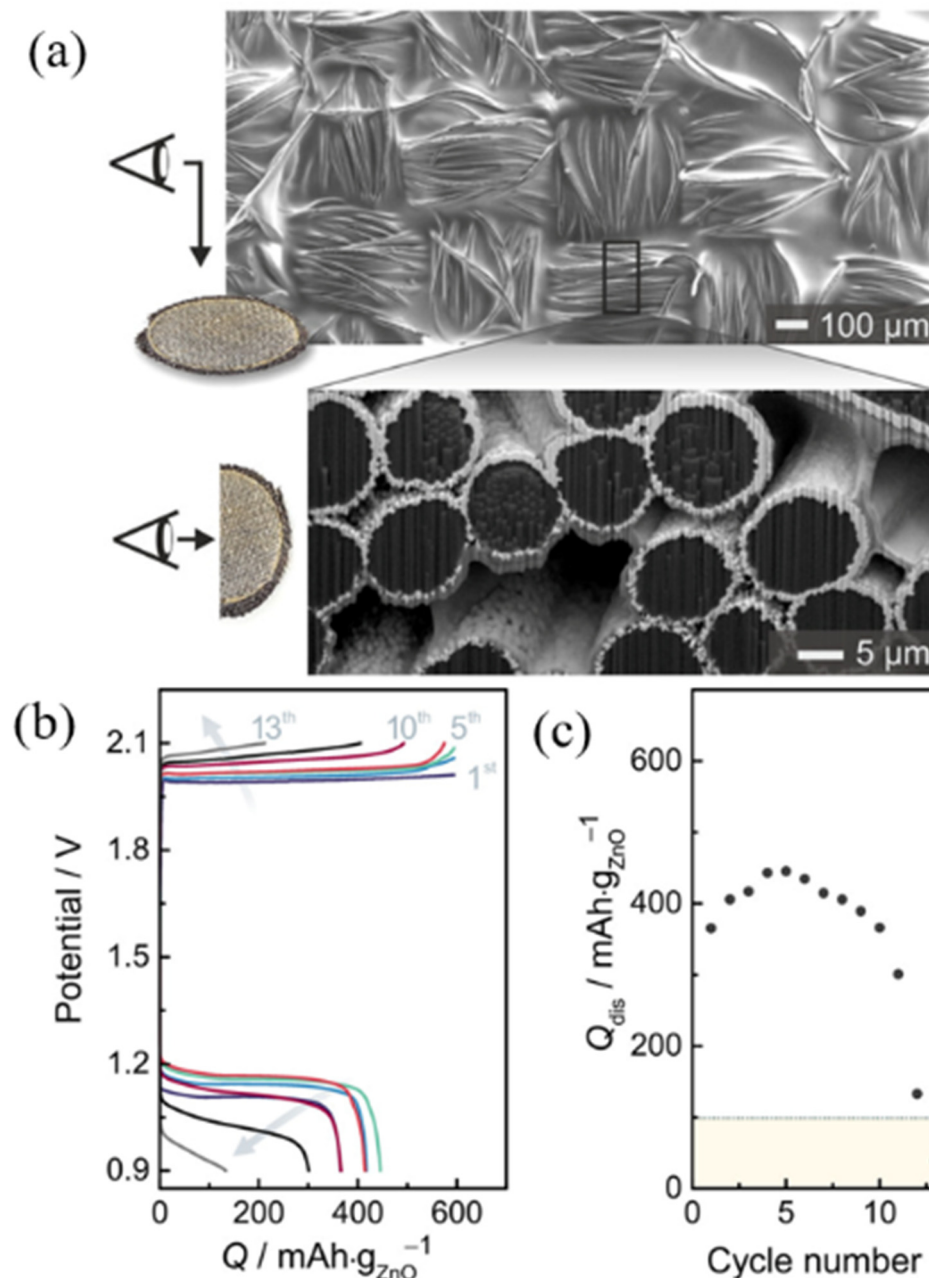


Figure 11. (a) SEM micrograph of FAA3-modified ZnO/C anode. The FAA3 is evenly distributed and coated over every carbon filament. (b) Charge/discharge profiles (in each cycle, charge and discharge curves are displayed with same color) (c) Specific discharge capacity Q_{dis} (derived using the electrodeposited mass of ZnO) with an averaged DoD of 53.6% for 13 cycles [53]. Reprinted with permission from Ref. [53], Copyright 2018, American Chemical Society.

However, one should be aware that the coating approach (organic and inorganic coatings) is still insufficient in improving the electrochemical activities and lifespan of the zinc anode. The inorganic coatings are fragile and break during zinc stripping/plating under long-term cyclization. The hydrophobic nature of the organic coating film may cause an extreme enhancement in polarization potential during zinc stripping/plating and an increase in the battery impedance by acting as insulators [55]. Figure 12 and Table 1 highlight the selection of works over the last five years on zinc anode optimization for the accomplishment of rechargeability in zinc–air batteries. Table 1 summarizes the articles discussed above, structural and surface optimization of the zinc anode, and their significant findings. Comparatively, structural optimization of zinc anodes seems to have more effect on enhancement in cycling stability and discharge capacity for zinc–air batteries. Zinc–air batteries investigation with high zinc utilization or deep DoD survives for fewer cycles. However, testing under deep DoD is necessary to evaluate the practicality of zinc anodes and compel high demand on their performance. Rechargeability corresponds to a highly reversible zinc anode with (i) a high percentage of operative material, (ii) the ability to efficient recharging, and (iii) the capacity could support many hundred charge/discharge cycles. Zinc anode structural optimization through alloying and electrodeposition, as well as surface optimization employing inorganic/organic additives coating, have been demonstrated to be effective measures for achieving the three requirements mentioned above. Most propitious additives are fruitful in minor quantities since a more fraction of additives minimizes the final zinc capacity. However, numerous research articles are published concentrating solely on estimating hydrogen evolution reaction (HER) suppression and corrosion inhibition without discussing comprehensive performance metrics, such as cycle stability, discharge capacity, and Coulombic efficiency. Thus, even more in-depth studies are needed to encourage durable anode reversibility for commercial applications.

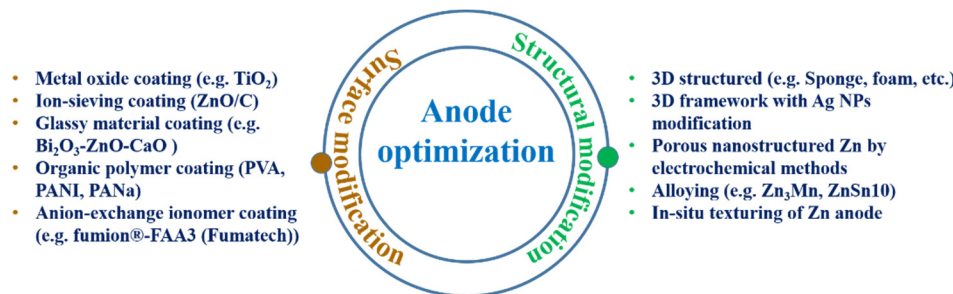


Figure 12. Schematic of anode optimization techniques.

Despite current achievements, still most zinc anodes' cycle lifespan is not as expected, mainly under deep discharge conditions. There are some evidence that >100 cycles of fully charge–discharge battery devices are achievable. To evaluate achievements of zinc anodes in zinc–air batteries, seven performance descriptors were proposed which should be reported in respective future research work and which would make different experiments comparable in a suitable way [40]. These were the (i) mass proportion of the operative or active material and anode composition (m_{AM}/m_{anode}), (ii) proportion of the capacity of operative material and quantity (volume) of electrolyte (Q_{AM}/V_E), (iii) the average utilization of active material (X_{AM}), (iv) mean Coulombic efficiency (Φ_Q), (v) the mean discharge capacity per mass of the anode composition (q_{dis}), (vi) the number of cycles (N_C), and (vii) outcome of mean discharge capacity per mass of the anode composition and the number of cycles ($N_C \times q_{dis}$). Alternatively, other metrics and perspective guidelines were given to evaluate claimed "breakthrough" results [56]. It is recommended to obtain the relevant results for electrolytes or electrode materials through full-cell prototypes where the measured parameters such as stable voltage window, round-trip efficiency, and the cycle life will reflect the assemblage conduct of all cell constituents involved. The interpretation of results would be preferable on superior zinc utilization (e.g., DoD~30–50%) with long-term cycle life rather than high number of cycle life with nominal zinc utilization (DoD~10–11%).

Though, the results with low zinc utilization and specific energy could not be considered as meaningless but may be balanced by adding other metrics such as volume-normalized energy density and cost benefits. Discussing these significant descriptors in future research studies would assist in evaluating the practical relevancy of zinc anodes for zinc–air batteries applications and permit credible comparison of diverse research investigations. This is significant for the speedy transport of zinc–air battery technical knowledge from mostly lab-based research to commercial or practical applications. In the forthcoming years, research goals should be to better active material utilization of zinc anodes (greater than 80%), improve Coulombic efficiency (greater than 80%), and ability to completely charge/discharge (DoD greater than 50%) with pertinent cycle life (greater than 500 cycles).

Table 1. Summary of research articles focused on zinc anodes optimization and a selection of their performance criteria (last five years).

Type of Anode Optimization	Anode Materials	Discharge Capacity/Areal Capacity	DoD/ZU	Cycling Stability	Coulombic Efficiency
Structural optimization	3D Zinc sponge anode [29]	164 mAh/g	23%	45 cycles (24 mA/cm ²)	-
Structural optimization	3D ZnO/C [17]	267 mAh/g	32%	60 cycles (0.55 mA/cm ²)	83%
Structural optimization	Ag-modified Cu foam/zinc [26]	-	20%	80 cycles (25 mA/cm ²)	94%
Structural optimization	Nanoporous zinc [30]	400 mAh/cm ²	10%	80 h (10 mA/cm ²)	
Structural optimization	Zn ₃ Mn alloy [31]	-		6000 min (30 mA/cm ²)	
Structural optimization	ZnSn10 [32]			200 h (0.5 mA/cm ²)	
Structural optimization	Textured zinc anode [38]	6 mAh/cm ²	20%	250 h (0.1 mA/cm ²)	
Surface optimization	ZnO@TiO ₂ [44]	- 616 mAh/g	40% 100%	170 cycles 33 cycles	93.09% 93.5%
Surface optimization	ZnO/C [46]	2.55 mA/cm ²	100%	42 cycles (2.55 mA/cm ²)	>95%
Surface optimization	Bi ₂ O ₃ –ZnO–CaO/Zn [48]	767 mAh/g	62%/ZU	20 cycles	
Surface optimization	ZnO/PVA/β-CD/PEG [51]	-		80 cycles (25 mA/cm ²)	
Surface optimization	PANI/Zinc-phthalocyanine [50]			120 h (10 mA/cm ²)	
Surface optimization	ZnO/C with FAA3 coating [53]	351 mA/g	53.6%	13 cycles	71.1

2.2. Electrolyte Optimization in Zinc–Air Secondary Cells

The contribution of electrolytes in metal–air batteries is equally significant for the zinc anode and air cathode side for secondary zinc–air batteries. The performance of zinc–air batteries mostly centers on the interaction between the electrodes and electrolytes. The type of electrolytes and their composition can affect the redox process and further impact the capacity and rechargeability of the batteries. [57]. With the growing attention to robust, flexible, good-performance, and rechargeable zinc–air batteries, research related to the progress of electrolytes is facing many possibilities. Aqueous alkaline electrolytes are widely used for zinc–air batteries because of their better results in context of interfacial properties and ionic conductivity. However, they are sensitive to CO₂ in the ambient atmosphere, generating unwanted carbonate precipitates and electrolyte degradation, thus prohibiting extended battery functionality and lifetime. The principal issues associated with zinc–air batteries with conventional aqueous alkaline electrolytes are zinc electrodes' high dissolution and corrosion. The high zinc dissolution leads to dendrite development, causing cell shorting. It will also lead to zinc electrode shape change, causing reduced capacity because of the reallocation of active material and thus diminishing the rechargeability. On the contrary, the zinc electrode's corrosion involves hydrogen evolution reaction on superficial zinc, which degrades zinc utilization. The other prominent issue related to aqueous electrolytes is water evaporation due to an air-exposed cathode, leading to electrolyte drying-out problems, including loss of ionic activity and battery performance. Leakage and extreme temperature functioning also lead to similar effects. In addition to electrolyte evaporation, the open-air electrode structure also results in carbonate formation due to the aqueous alkaline electrolytes' sensitivity towards CO₂ exposure. The CO₂ from

atmosphere reacts with hydroxide present in electrolyte leading to bicarbonate/carbonate anion generation. Aqueous alkaline electrolyte carbonation will decrease ionic activity because carbonate and bicarbonate anions have lower movability compared to hydroxide ions. The carbonate deposition may plug holes in the air electrode and increases the electrolyte's density, which will obstruct oxygen diffusion, leading to lethargic kinetics for OER/ORR. These problems will result in zinc–air batteries with diminished capacity and cycle life. To combat electrolyte evaporation and carbonate formation issues, researchers have reported different strategies related to the optimization of the concentration and composition of the electrolytes. For instance, water-retaining additives (e.g., silica), polymer gel electrolytes, and ionic liquids help in minimizing electrolyte evaporation [58,59]. On the other hand, using electrolyte additives (e.g., K_2CO_3) in alkaline electrolytes, neutral aqueous electrolytes, and neutral polymer gel electrolytes and molten salt electrolytes helps mitigate carbonate formation [60–62].

Thus, one of the critical aspects of extending the cycle life of zinc anode is selecting the appropriate electrolyte system and, therefore, adequately upgrading its rechargeability. The current methods to alleviate significant zinc anode problems have been chiefly focused on employing additives in the electrolyte and zinc electrode. For instance, in a recent report, choline chloride as an additive in an aqueous $ZnCl_2$ electrolyte increases zinc plating/stripping efficiency [63]. The quaternary ammonium cations of choline chloride superficially adsorb on the zinc electrode, hindering zinc dendrite growth. On the other hand, hydroxide ion moieties of choline chloride disrupt hydrogen bonds in aqueous electrolytes, decreasing water activity and mitigating water-based side reactions. As an alternative, special consideration was given to other aqueous neutral and non-aqueous electrolytes (comprising solid-state electrolytes and room-temperature ionic liquids) [64–66]. While a detailed discussion on electrolytes and their performances goes beyond the scope of this article; however, optimization of aqueous electrolyte pH and its composition is another strategy to improve zinc utilization and rechargeability and should be highlighted here with respect to some very recent developments opening new avenues (Figure 13).

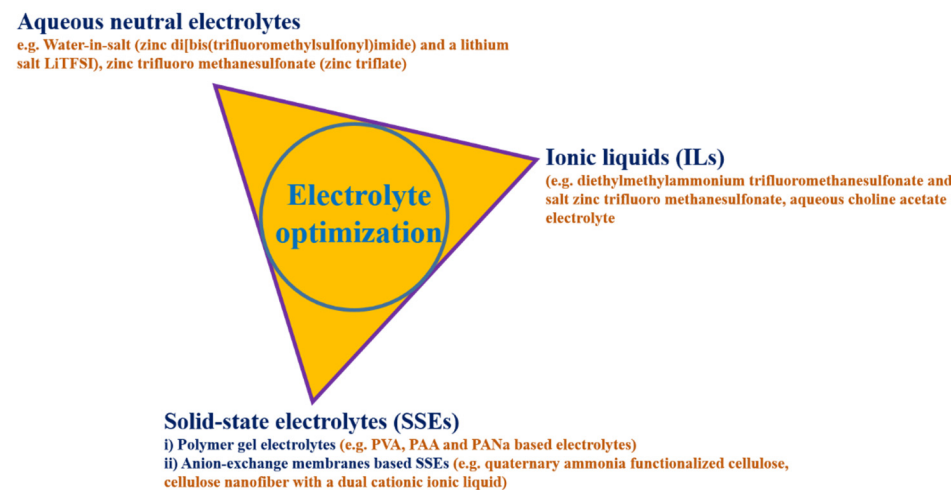


Figure 13. Schematic for recent electrolyte optimization techniques for zinc–air batteries.

2.2.1. Aqueous Neutral Electrolytes

In aqueous neutral electrolytes, zinc anode and air cathode are stable because of low zinc solubility and slow carbon dioxide absorption, which hinder zinc dendritic growth and carbonate generation [10]. However, zinc is not much active in neutral electrolytes, and oxygen redox reactions at the air electrode are moderate. Thus, water-in-salt electrolytes (WiSE), a type of quasi-neutral electrolyte, has prompted immense interest recently. For instance, highly concentrated zinc-ion electrolyte $1\text{ m Zn(TFSI)}_2 + 20\text{ m LiTFSI}$ (m is molality (mol/kg), Zn(TFSI)_2 is zinc di[bis(trifluoromethylsulfonyl)]imide), and LiTFSI is the lithium salt which is neutral in pH and highly concentrated with a supporting salt,

and can retain water in an open atmosphere and assist efficient zinc plating/stripping without any dendrite formation [67]. The zinc–O₂ battery assembly delivers >200 cycles of activity and an energy density of 300 Wh/kg. The high zinc reversibility is attributed to the Zn²⁺ solvation-sheath structure in the overly condensed aqueous electrolyte. The excessive concentration of TFSI⁻ anions encourages the formation of close-packed ion pairs (Zn-TFSI)⁺ and significant suppression of [Zn (H₂O)₆]²⁺. Thus, retention of water electrolyte and suppression of zinc hydroxide formation reduces parasitic side reactions such as dendrite formation or HER, leading to high zinc utilization. Even though WiSEs are initially considered widely in metal-ion batteries. The above-mentioned introductory work has illustrated their adaptability and electrochemical achievement in a metal–air battery, encouraging the durability of WiSE electrolytes and inspiring novel frontiers in developing neutral Zn-air batteries.

Recently, the use of non-alkaline quasi-neutral zinc trifluoromethanesulfonate (zinc triflate or Zn(OTf)₂) electrolyte, which has a large fluorinated anion, has been reported in the zinc–air battery system. The OTf⁻ ions act as water repellent creating a zinc ion-abundant Helmholtz layer across the air electrode, encouraging eminently reversible redox reactions and averting water-related side reactions (Figure 14a). The cell process proceeds through zinc peroxide chemistry via a two-electron ORR instead of a four-electron pathway typically operating in the zincate-based cells. In alkaline KOH electrolyte, the Zn–air battery lasted 3 and 12 cycles in ambient air and neat O₂, respectively. In contrast, the zinc–air battery with Zn(OTf)₂ electrolyte exhibits similar performance in ambient air and neat O₂. The non-alkaline ZnSO₄ electrolytes are also considered as alternatives to KOH electrolytes with better electrochemical properties. Figure 14a,b display the scheme for two electron and four electron reaction pathways in Zn(OTf)₂ and ZnSO₄ electrolytes, respectively. The zinc–air battery with ZnSO₄ electrolyte shows a continuous increase in pH over discharging (ORR) and a decrease over charging (OER) due to the generation of OH⁻ ion during ORR and consumption of OH⁻ ion during OER, whereas zinc–air battery with Zn(OTf)₂ electrolyte retain a steady pH in both the charge (OER) and discharge (ORR) process (Figure 14c). Further, the ZnSO₄-based zinc–air cell shows the formation of zinc sulfate hydroxide (ZSH) during discharge. The formed ZSH has a large flake-like structure, a part of ZSH passively deposited due to its poor reversibility in the ZnSO₄ electrolyte. Whereas in the case of Zn(OTf)₂ electrolyte, the discharge product is ZnO₂ which has a fibrous structure (~100 nm). During charging, ZnO₂ completely vanishes, exhibiting its electrochemical reversibility. Moreover, the zinc–air cell with Zn(OTf)₂ electrolyte exhibits stable 320 cycles of activity at 1 mA/cm² (Figure 14d). Thus, quasi-neutral electrolytes with 2e⁻ pathway open a new area of research as solution to electrochemical irreversibility not only in zinc–air but also in other metal–air batteries. However, it is essential to understand that the two-electron pathway involves peroxide species that could corrode carbon-based catalysts because of their oxidization property. So, this may create new pitfalls on the air electrode side of the zinc–air battery. Thus, the catalyst composition for the air electrode must be precisely selected, and a more extensive understanding of the two-electron oxygen chemistry is essential. [68]. The performance based on anode modification (3D anodes) and non-alkaline electrolytes are inspiring, but an actual device still needs optimization.

Since zinc–air batteries are supposed to be functional in an open-air atmosphere, electrolyte evaporation is unavoidable. Solid-state electrolytes (SSEs) and ionic liquids (ILs) are effective alternatives and solutions to solve the evaporation problem [69].

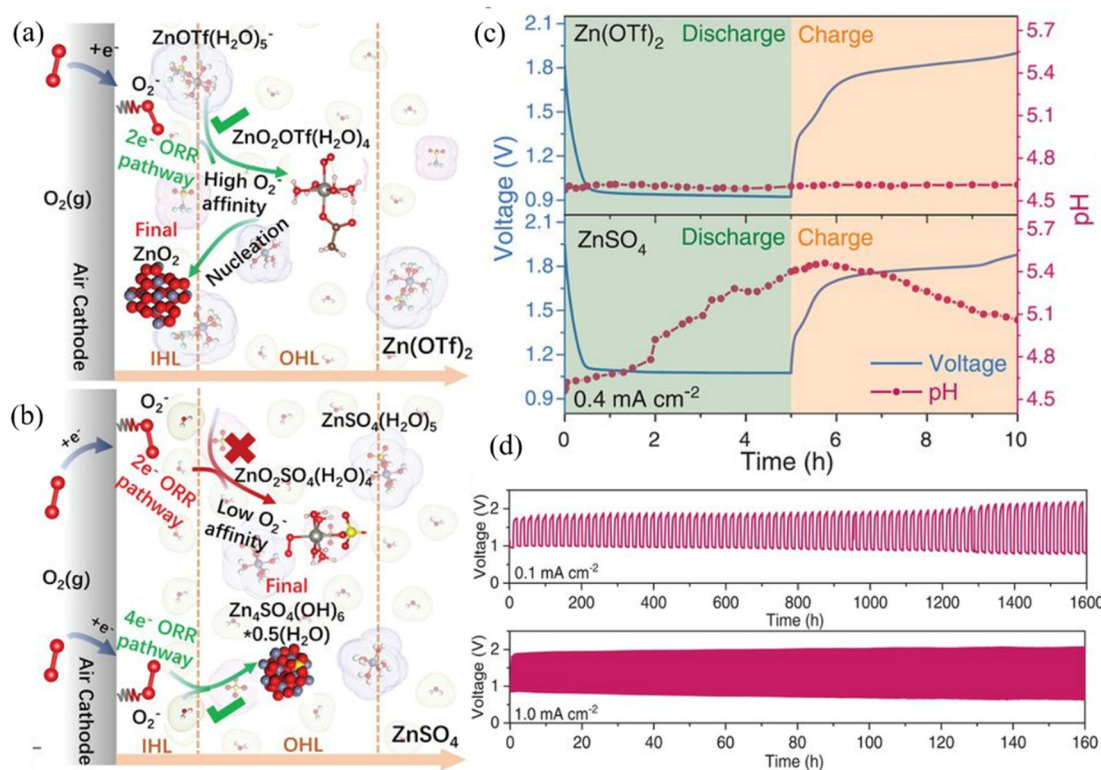


Figure 14. Schematic representation of reaction process in the inner Helmholtz layer (IHL) and outer Helmholtz layer (OHL) across the external surface of the air electrode in (a) Zn(OTf)₂ (two-electron) and (b) ZnSO₄ (four-electron) electrolytes, respectively; (c) Galvanostatic charge/discharge curves of Zn-air cells prepared with Zn(OTf)₂ and ZnSO₄ electrolytes at a current density of 0.4 mA/cm² and the corresponding noted pH values of the electrolyte, (d) long-duration cyclic activity of Zn-air cells at 0.1 and 1.0 mA/cm² current densities. [68]. Reprinted with permission from Ref. [68], Copyright 2021, AAAS.

2.2.2. Solid State Electrolytes (SSEs)

SSEs have gained attention for acquiring properties such as thermal stability, mechanical stability, and ionic conductivity. Due to these characteristics, zinc–air batteries with solid-state electrolytes have widened the scope of implementation, including flexible, portable, and various-shaped devices. SSEs reported for zinc–air batteries can be mainly categorized in polymer gel electrolytes (PGEs) and anion-exchange membrane (AEM) based SSEs. Solid electrolytes act as a better alternative to reduce issues of zinc corrosion, shape change, and dendrite growth while using aqueous alkaline electrolytes [70]. However, SSEs suffer frontier resistance between SSEs and zinc electrodes, leading to small reversibility and degradation in the battery's lifetime. Therefore, SSEs combine the benefits of both solid and liquid electrolytes, consequently quasi-solid-state PGEs have been introduced. PGEs were prepared by gelatinizing an alkaline solution (e.g., KOH) with low molecular weight polymers (e.g., PVA, PAA and PANA). PGEs provide energy storage devices with flexibility and adaptable shapes, which is favorable for portable and wearable electronics [71,72]. Although PVA (polyvinyl alcohol)-based gel electrolytes have been considerably explored, the latest research focusses on polymer gels such as PANA (poly sodium acrylate), PAA (polyacrylic acid), and PAM (polyacrylamide) which promises better electrochemical performance.

For instance, PVA based alkaline porous PGEs was reported for flexible sandwich type zinc–air batteries [73]. The porous PVA-based alkaline PGE was prepared by the addition of 5 wt% SiO₂ and displayed eminent ionic conductivity (57.3 mS/cm) and enhanced cycle-life of 144 cycles (~48 h testing time) surpassing the conventional PVA–KOH PGE system. This is due to the increase in ionic conductivity and electrolyte retention capability of the PGEs. Furthermore, high performance PGEs were fabricated by multiple crosslinking reactions

between PVA, PAA, and graphene oxide with KI additive (PVAA-GO) [74]. The hybrid polymer hydrogel displayed improved water holding capacity and alkali uptake capacity in contrast to the conventional PVA gel. The zinc–air battery fabricated using this PVAA-GO PGE displayed superior ionic conductivity of 155 mS/cm and a stable cyclization up to 200 cycles (~200 h) with high energy efficiency (73%). Moreover, a secondary zinc–air battery displayed high reliability under harsh working conditions and excellent flexibility when integrated into wearable electronic devices.

Gelation of ingredients frequently hinders ionic conductivity in the solid state electrolyte, immensely hydrophilic and alkaline resistant additives such as cellulose, quaternary ammonium and KI, are usually used with PGEs to increased their stability and ionic conductivity [75]. For instance, PANa-based electrolytes with quaternary ammonium functionalized cellulose additives favor a solid electrolyte interface that enables uniform ion transfer and assists in dendrite-free, stable battery performance (800 cycles/160 h) [76]. Polymer gel electrolytes have widened application in solid state zinc–air batteries; however, they suffer from the uncertainty of battery failure due to KOH leakage, poor mechanical stability and low ionic conductivity [77]. Though solid-state zinc–air batteries are safer than volatile liquid batteries, however practical use of polymer gel electrolytes in zinc–air batteries is not workable because of low dissolution of zinc salts and the often volatile nature of the organic solvents used.

Anion-exchange membranes (AEMs) act as a risk-free hydroxide ion conductor because it transfers hydroxide ion through cation groups thus avoiding corrosive KOH solution. Lately, a number of AEM-based SSEs (AEM-SSEs) have been investigated in zinc–air batteries, such as graphene oxide, polyvinyl alcohol, chitosan and quaternary ammonium functionalized cellulose [75,78–81]. Nevertheless, AEM-based SSEs similar to PGEs also suffers from deficitary water uptake and retention, low ion conductivity and mechanical stability. Recently, cellulose based AEM-SSEs have received considerable attention because of its hygroscopic, earth abundant, and environmental benign characteristics. They are also better in restricting volume expansion and improving mechanical stability in context to polymer gel electrolytes. Thus, many celluloses and modified celluloses possessing enhanced hygroscopicity and high crystallinity have been used as AEM-SSEs in zinc–air batteries. For instance, quaternary ammonium functionalized cellulose (QAFC) as AEM-SSEs for a rechargeable zinc–air battery (Figure 15a) [75]. The QAFC membrane possess various sized cellulose fibers comprising nano/micro-fibers and micron-sized fiber bunches. The assembly and functioning of the zinc–air battery is described in Figure 15a. During charging, OER takes place at the air electrode with the help of OH[−] generated at the zinc electrode and transferred through the QAFC membrane. During discharge, zinc oxide formed due to an interaction between zinc and hydroxide ions migrated through the 2-QAFC membrane from reaction sites on air electrodes. The surface functionalization process of cellulose nanofibers is shown in Figure 15b. Dimethyloctadecyl [3-(trimethoxysilyl)propyl] ammonium chloride (DMOAP) was used as a precursor for quaternary ammonia (QA) functionalization. The quaternarization process involves the formation of hydrolyzed silanol moieties and their adsorption on the surface of cellulose nanofibers by hydrogen bonding (step 1). Further, the crosslinking process involves heat treatment, and hydrolyzed silanol groups interact with OH[−] of cellulose, resulting in the formation of (Si–O–C) and (Si–O–Si) (step 2). Thus, covalent crosslinking is established between functional moieties and the cellulose nanofibers, ensuring enhanced dimensional stability of the membrane. Finally, the functional moieties incorporated on the membrane were alkaline exchanged by treatment with KOH, which provides membrane hydroxide ion conductivity (step 3). The solid–state zinc–air battery’s cyclic behavior of 2-QAFC membrane (prepared using 200 mol% of concentration of DMOAP) is better in comparison with commercial available alkaline anion-exchange membrane (A201) as shown in Figure 15c. The batteries were cycled at current density of 250 mA/g with 60 min of each charge/discharge cycle (25% DoD). The battery with A201 deteriorates in 720 min whereas battery with 2-QAFC membrane lasted more than 2100 min without any degeneration

in charge and discharge. This excellent cycling stability of 2-QAFC is due to its superior hydroxide ion conductivity (21.2 mS/cm) along with high water holding capacity due to its nanoporous structure and low anisotropic swelling, which assist it to bear the periodic stress and dehydration during charge and discharge process. Figure 15d displays the effect of CO₂ on zinc–air battery performance with 2-QAFC membrane. The cell in O₂/CO₂ mixture supply, show higher polarization due to carbonate formation. However, after 420 min, it shows similar polarization to the zinc–air cell when cycled under pure O₂ supply.

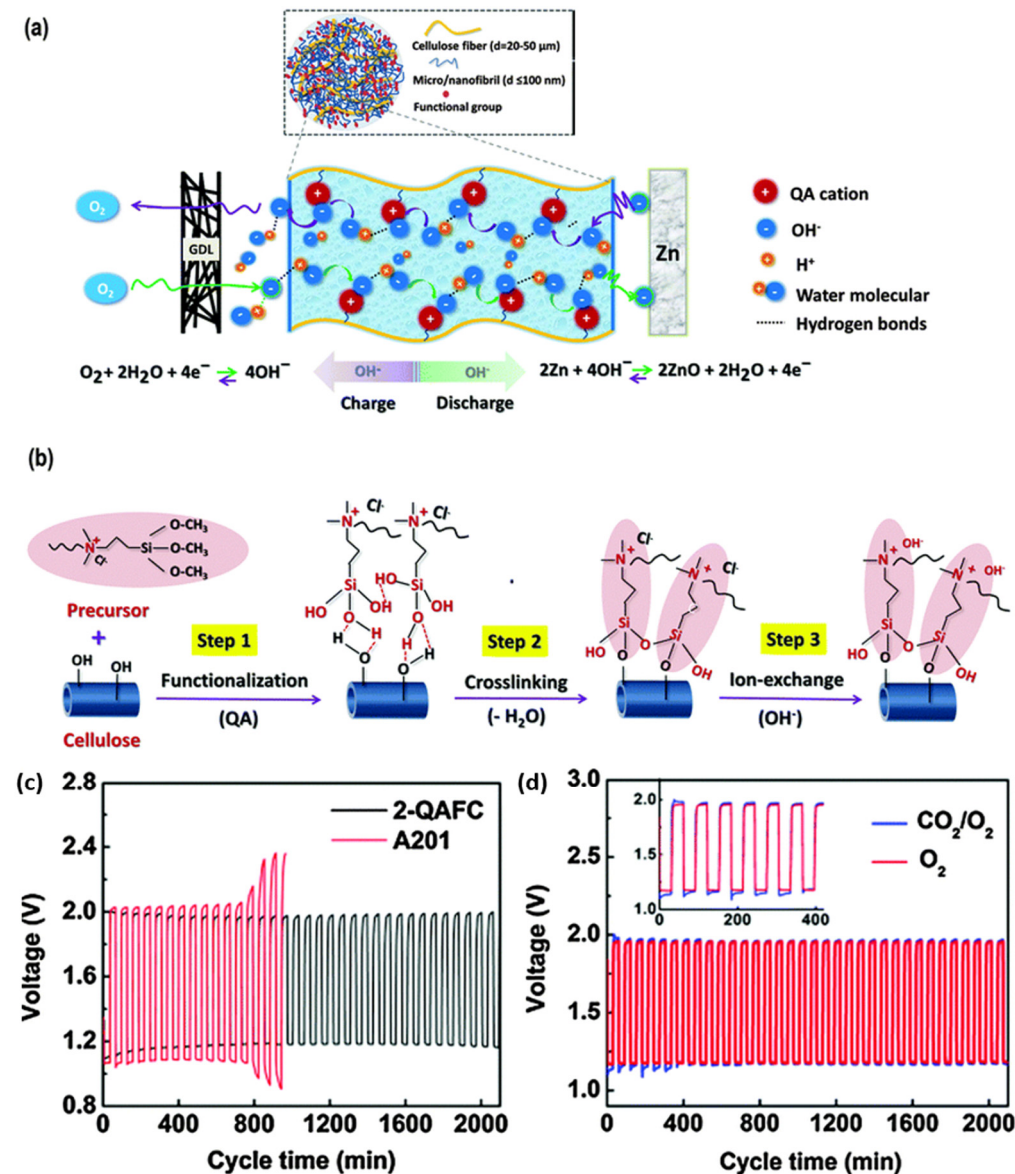


Figure 15. (a) Schematic representation of rechargeable zinc–air battery fabricated employing solid-state electrolyte QA–functionalized nanocellulose membrane layer. (gas diffusion layer (GDL); QA: quaternary ammonium) (b) Stepwise structural development of the cellulose nanofibre superficial layer including functionalization, cross-linking and hydroxide ion-exchange. (c) Charge/discharge cyclization of zinc–air batteries fabricated using 2–QAFC and A201 membranes with 60 min each cycle time at 250 mA/g current density (d) Charge/discharge cyclic performance of the zinc–air battery in the presence of neat oxygen and 20,000 ppm CO₂ contaminated gas reactants, respectively, with 60 min each cycle time at a current density of 250 mA/g [75]. Reprinted with permission from Ref. [75], Copyright 2016, The Royal Society of Chemistry.

Recently, a novel hierarchically nanostructured cellulose-based SSE was fabricated by nano-confined polymerization of three dimensional porous cationic cellulose nanofiber (CCNF) employing a dual cationic ionic liquid (PDIL) [82]. The dual cationic ionic liquid is designed to obtain higher cationic density than that of conventional AEMs. The resulting solid electrolytes CCNF–PDIL have plenty of ion-conductive nano-channels due to the use of a ,3D porous CCNF and dual cationic IL. It also exhibits robust mechanical strength due to reinforced concrete architecture formed 3D CCNF skeleton and strong noncovalent interactions between CCNF and PDIL. The CCNF–PDIL solid electrolyte exhibit mechanical durability, good flexibility, considerable water uptake and high ion conductivity of 286.5 mS/cm. The fabricated solid-state flexible zinc–air battery displayed an improved power density of 135 mW/cm² and a cycling stability of 720 cycles (240 h). It also depicts good flexibility at different bending states (0°, 45°, 90°, and 180°) and display steady charge–discharge voltage plateau.

Talking of practical applications, a realistic zinc–air pouch cells was recently fabricated using chitosan-biocellulosics (CBCs) as SSE with copper phosphosulfide (CPS(101)) as a cathode and patterned zinc metal as anode (Figure 16a–d) [83]. The anti-freezing chitosan-biocellulosics superionic conductive electrolytes (CBC-SCEs) were fabricated by joining of partially oxidized CBCs and quaternized CBCs. The CBC-SCEs exhibit high hydroxide ion conductivity of 86.7 mS/cm at 25 °C with eminent chemical and mechanical durability due to which the fabricated flexible zinc pouch cell (ZPC) operates efficiently in between –20 to 80 °C temperature range. The ZPC exhibit energy densities of 460 Wh/kg_{cell} and 1389 Wh/l with a long life span (6000 cycles at 25 mA/cm², Figure 16e) and display cyclic stability of >1100 cycles at high DoD (70%, 25 mA/cm²). It depicts high durability and rechargeability under practical conditions interesting for possible commercial applications (Figure 16f). It also depicts good flexibility at distinct bending angles (0°, 90°, 180° (folding) and 0°) and display stable charge–discharge voltage plateau (Figure 16g).

Moreover, enhanced contact between the metallic zinc anode and SSE can resolve the issue of interfacial resistance. Recently a new strategy was reported to optimize the zinc electrode/solid-state electrolyte interface by integrating a porous zinc electrode and a thermal-sensitive solid-state electrolyte. The porous zinc anode prepared by electrodeposition of zinc on a zinc substrate reduces zinc passivation and improves the rate of zinc utilization. The F127 surfactant was used as a solid-state electrolyte to improve the contact between SSE and zinc anode due to its low-temperature fluidity. Due to the porous anode structure and improved contact, the fabricated solid-state zinc–air battery exhibits an area capacity of 133 mA/cm², which is 100 times better than the solid-state battery fabricated with conventional zinc foil anode [84].

For flexible solid-state batteries, a stable electrochemical performance under irregular external forces is essential for their commercial application. SSEs have gained much attention due to the increasing recognition of flexible electronics. In batteries, extensive research is underway for developing SSEs (especially PGEs and AEM-SSEs) with improved energy density, flexibility, and dependability. However, these OH[−] conducting SSEs depict less power functioning and inferior cycling stability than their aqueous equivalents due to low anode utilization, interface stabilization issues, and preservation of physical contact [85,86]. SSEs can retain a small amount of zincate ion; thus, zincate converts to ZnO, whose accumulation can block SSEs leading to low zinc utilization. The second obstacle is the stabilization of interfaces. The interfacial construction and composition between electrodes and SSEs is different from those of aqueous electrolytes. The development of ionically non-conductive decomposition products has hindered solid-state batteries operating regime. Explaining the interface characteristics will help to establish a reasonable perspective toward the arrangement of materials in the next generation of solid-state batteries. The third obstacle is resistance in ion transport in SSEs and solid-state batteries due to insufficient physical contact between solid particles. The solution to these obstacles depend on a further and even, more detailed understanding of the fundamental properties of solid state electrolyte materials.

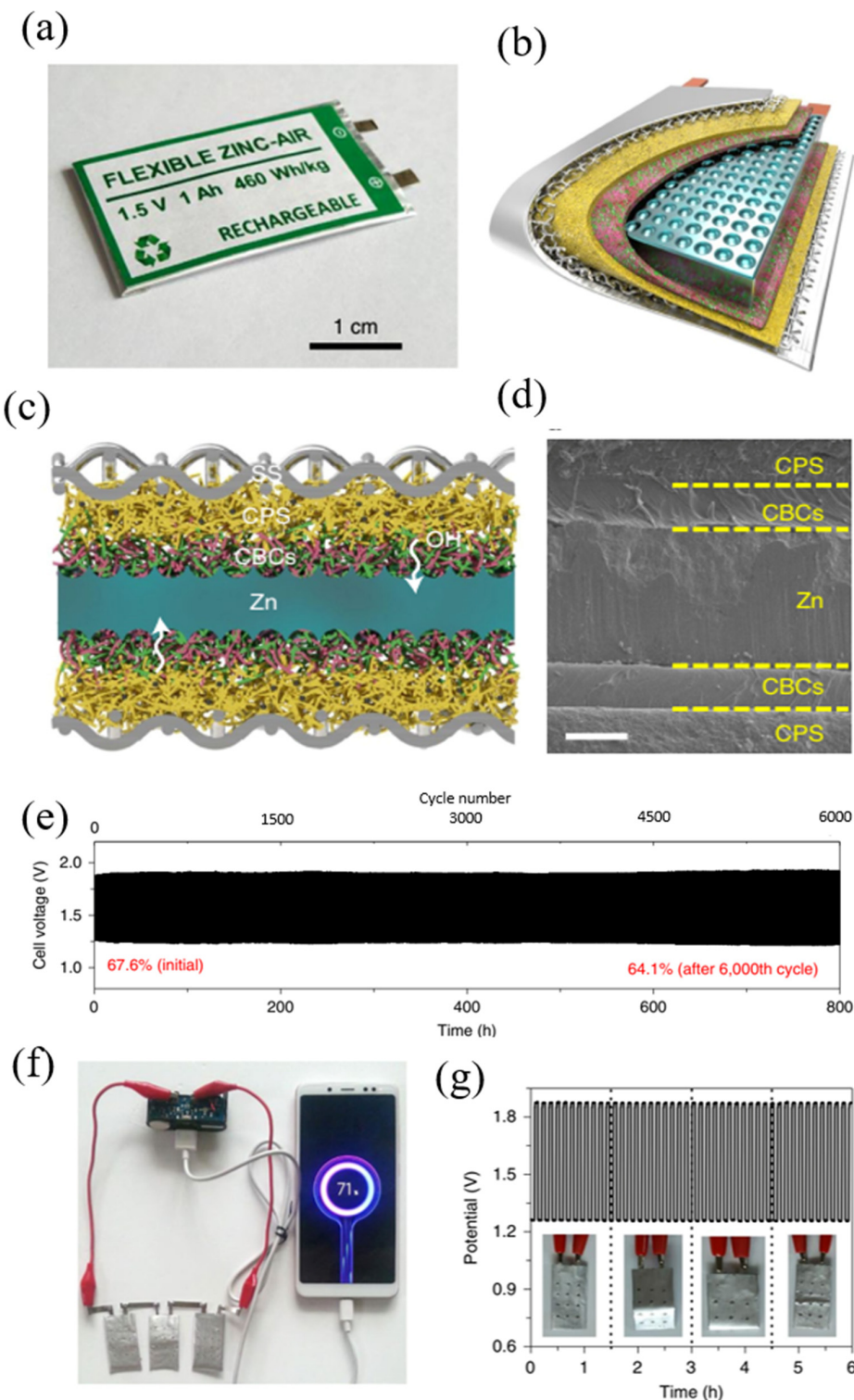


Figure 16. (a) A photo-picture of zinc–air pouch cell. (b), graphic scheme dissecting a layered construction of the pouch cell, (c,d) a cross-sectional representation, (c) exhibiting the uniformly ordered cross arrangement with [CPS(101) || CBCs || patterned zinc || CBCs || CPS(101)] and (d) the related cross-sectional SEM micrograph, (e) cyclization of CPS(101) || CBCs || patterned zinc || CBCs || CPS(101) at current density of $25\text{ mA}/\text{cm}^2$. The percentile values display the potential effectiveness of the cells. (f) Display 3 pouch cells charging a smartphone (threshold voltage of 4.5 V) and (g) Charge/discharge cyclic performance under distinct bending angles (0° , 90° , 180° (folding) and 0°) at $25\text{ mA}/\text{cm}^2$ [83]. Reprinted with permission from Ref. [83], Copyright 2021, Springer Nature.

2.2.3. Ionic Liquid Electrolytes

Ionic liquids (ILs) are regarded as a promising class of electrolytes due to their highly stable, non-volatility, and broad electrochemical window characteristics. Thus more attention has been paid to ILs as an alternative to alkaline electrolytes [87]. Applying ILs as the electrolyte in zinc–air batteries can beneficially resolve the problems of electrolyte evaporation, CO₂ destruction, and zinc anode degradation. Furthermore, aprotic ILs, can effectively inhibit the corrosion of the zinc anode triggered by HER [88]. Thus, ILs as an electrolyte for zinc–air batteries have been considered in recent years. In conventional aqueous alkaline electrolytes OH[−] ions are required in both the zinc and air electrode reactions; however, the fundamental electrochemistry of rechargeable zinc–air batteries based on ILs is somewhat different and dependent on the character of the constituent anions and cations [89]. In the zinc–air cell with appropriate ILs as an electrolyte, zinc oxidizes to Zn²⁺ in a reversible reaction. However, if the combination is inappropriate, ILs may form an insoluble complex with zinc leading to irreversibility. The ORR/OER in the presence of ILs involves a reversible two-electron process with stable peroxide products [89]. Moreover, ILs as electrolytes in rechargeable zinc–air batteries still face several challenges, such as high cost hindering its large-scale applications. The ILs show low conductivity because of the low mobility of ions which in turn is due to high viscosity resulting in poor electrochemical activity at both zinc and air electrode. Thus IL-based rechargeable zinc–air batteries deliver low energy density and can only operate at low current density. To increase conductivity and electrochemical performance, ILs together with some additives (water and salts) as electrolytes have recently been explored in zinc–air battery systems [64,90]. For instance, diethylmethylammonium trifluoromethanesulfonate (DEATfO), an IL mixed with a salt zinc trifluoro methanesulfonate as the electrolyte, zinc metal as the anode, and Pt/C as catalyst on the air electrode side are promising [64]. The fabricated rechargeable zinc–air battery shows a stability of up to 700 h without any noticeable change in cell potential, and there was no zinc dendrite formation. However, the maxima cell power density (45 µW/cm²) was comparably low, which is because of the low wetting property of the ionic liquid. Recently, aqueous choline acetate (ChAcO) as an electrolyte and MnCo₂O₄ as a bifunctional catalyst on the air cathode was reported in the fabrication of rechargeable zinc–air batteries exhibiting promising results [91]. The aqueous ChAcO mixture (30 wt.%) exhibits high contact angles similar to alkaline KOH electrolytes with pH value and conductivity of 10.8 and 5.9 mS/cm, respectively. Zinc–air battery cycled for 100 h charge/discharge at 100 µA/cm² realizing a reversible capacity of 25.4 mAh (28% DoD) with energy efficiency between 29 to 54% during the 1st and 7th cycle in a 1500 h polarization duration. Because of the high pH value of around 11 of aqueous ionic liquid, zinc–air cell reaction products such as ZnO and zinc hydroxide are similar to those reported in alkaline KOH. However, in contrast to reactions in KOH, neither carbonate nor zinc dendrite development was seen in the choline acetate electrolyte. Furthermore, other ILs should be explored in zinc–air batteries, comprising the beneficial impact of additives in ILs. It is also essential to discover suitable bifunctional catalysts for air electrode which can lower the energy barrier of ORR/OER with such IL-electrolytes. Even though the IL-electrolytes require further studies concerning interface properties, the transfer mechanism of active substances and redox reaction efficiency suggest that ILs are beneficial electrolytes for zinc–air batteries [59,69].

2.2.4. Wide Working Temperature

Extreme temperature working conditions are essential for energy-harnessing applications at maximum altitudes, longitudes, and deep seas. Operation of zinc–air batteries with open-air electrodes is affected by temperature variation because electrocatalytic activities are vulnerable to temperature, as demonstrated in the Arrhenius equation [92]. At lower temperatures, OER and ORR are influenced explicitly due to the involvement of several oxygen intermediates in the reaction and the aqueous nature of the electrolyte in zinc–air batteries [93]. Most of the research on zinc–air batteries are reported at room temperature.

This section focusses on research work displaying wide working temperatures for zinc–air batteries. For instance, the extreme temperature (-30 to 80 $^{\circ}\text{C}$) functioning of a flexible zinc–air battery was feasible by considering the improvement in interaction among solid active catalyst, liquid electrolyte, and gaseous oxygen at triple phase interphase in the vicinity of the cathode [94]. The strategically developed stereoscopic optimized planar electrocatalyst-electrolyte interface enhances the triple-phase interface's adaptability to extreme temperature changes. A fibrous carbon electrode was prepared by electrodeposition of polypyrrole on carbon cloth, generating a number of active sites. The air electrode was fabricated by incorporating Co^{2+} and Fe^{3+} salts through pyrolysis and phosphatization on the surface of the fibrous carbon electrode. The process stabilized the active metal species, which acts as an efficient bifunctional catalyst. Afterward, carboxylate groups were incorporated in alkaline polyacrylate hydrogel with 30% KOH to fabricate flexible polyelectrolytes. Eventually, the assembled zinc–air battery exhibits cycling efficiencies of 69.9% at 80 $^{\circ}\text{C}$, 60.4% at 30 $^{\circ}\text{C}$, and 65.9% at 25 $^{\circ}\text{C}$, displaying less sensitivity to temperature changes (Figure 17a). In a similar report, a flexible zinc–air battery assembled with bamboo-like structured electrocatalyst and hydrogel electrolyte possessing anti-freezing properties displayed retention of about 87.2% of energy density and 92.7% of capacity on decreasing the working temperature from room temperature to -20 $^{\circ}\text{C}$ [72].

Flexible solid-state and quasi-solid-state zinc air batteries are mostly studied for extreme temperature ranges [72,93–96]. However, in a very recent study aqueous alkaline zinc–air battery displayed promising result at subzero temperatures [97]. At subzero temperature decrease in electrolyte conductivity and the resultant increase in internal resistance is the central limiting aspect for low-temperature zinc–air batteries. Theoretical simulations and experimental studies established the usability of high-concentration alkaline electrolytes in zinc–air batteries at low-temperature and the electrode's unresponsiveness towards temperature changes. A sequence of alkaline electrolytes involving 0.20 M Zn(OAc)_2 and 6.0 M MOH and ($\text{M} = \text{Li}, \text{Na}, \text{K}, \text{Rb}, \text{Cs}$; 5 M of LiOH because of its less solubility). It was concluded that except LiOH, all other electrolyte exists in a liquid state even at -30 $^{\circ}\text{C}$. The conductivity of the electrolyte at low temperatures follows order $\text{Cs} > \text{Rb} > \text{K} > \text{Na} > \text{Li}$, indicating the ability of CsOH-based electrolytes to support low-temperature zinc–air batteries. The assembled zinc–air battery exhibits a 500-cycle lifetime with a steady potential gap of 0.8 V at 5 mA/cm^2 at a working temperature of -10 $^{\circ}\text{C}$ (Figure 17b).

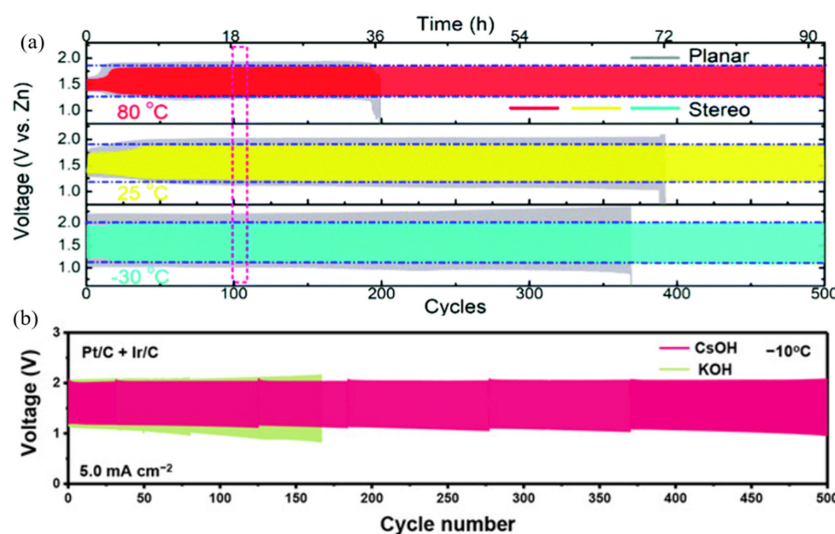


Figure 17. (a) Cyclization profile of stereo (red, yellow and green) and planar (grey) electrodes fabricated zinc–air batteries at varying temperatures, at 2 mA/cm^2 , Reprinted with permission from Ref. [94], Copyright 2021, The Royal Society of Chemistry. (b) Cyclization profile of zinc–air battery with CsOH-based electrolyte at -10 $^{\circ}\text{C}$, at 5 mA/cm^2 . Reprinted with permission from Ref. [97], Copyright 2021, John Wiley and Sons.

2.3. Solid Electrolyte Interphase (SEI) in Secondary Zinc Air Batteries

In batteries, the electrolytes enable fast ion diffusion in bulk and thus endorse high power density storage. However, the anodes often degrade due to their chemical and physical interactions with the electrolyte over time, decreasing safety and battery lifetime. One of the effective methods to improve zinc anode reversibility is to create a firm and durable SEI along the vicinity of the zinc anode surface. However, non-uniform and unstable SEI may also lead to non-uniform deposition leading to dendritic growth [98–100]. The SEI can be developed either by *in situ* formation of ion-mediated interphase or *ex situ* deposition of materials such as inorganic compounds, polymers, and metal-organic frameworks [38,101,102]. An *in situ* SEI is a composite (organic/inorganic) passivation layer produced near the electrode surface in proximity to liquid electrolytes containing salts, additives, and solvents during electrochemical reactions [103]. Nevertheless, surprisingly little has been reported on the chemical nature, stability, and functionality of the SEI in zinc-air batteries [5,103]. The issues of irreversibility in zinc-air batteries could be resolved by better understanding SEI formation onto zinc anodes. However, SEI on zinc anodes is unfeasible due to the anions of the zinc salt being electrochemically very stable in solution and not developing a stable SEI [104,105]. The concept could be realized by taking the example of SEI development in lithium metal batteries, where usually electrolyte is an organic solvent mixed with a lithium salt. Lithium has a low reduction potential of -3.04 V vs. SHE, which gives it a vulnerability to oxidize readily in contact with electrolytes leading to the formation of self-generated SEI. In contrast, zinc is comparatively stable in both aqueous and organic electrolytes (high redox potential of -0.76 V vs. SHE), which means spontaneous generation of the SEI in zinc metal batteries is insignificant [104]. For aqueous zinc anodes, a competitive H_2 evolution reaction unavoidably occurs during each recharging cycle, and also local pH change instigates the formation of ionically non-conducting by-products, making *in situ* SEI formation impractical [106,107]. Nevertheless, in case of zinc-ion batteries *in situ* Zn^{2+} -conducting SEI was reported in non-aqueous electrolytes [106,107] and water-in-salt electrolytes (WiSE) [67]. In non-aqueous/organic electrolytes, SEI between electrolyte and electrode surfaces are created during initial charging by sacrificial electrolyte decomposition, and these interphases are composed of a barrier permitting ionic conduction but prohibiting electronic conduction [108]. The existence of SEI considerably enhances the electrochemical functional window of electrolytes. In traditional aqueous electrolytes, a protecting interphase is non-existent because the decomposition outcomes of water (OH^- , O_2 , or H_2) cannot deposit as solid-state interphase. In the case of WiSE, for instance, electrolyte is obtained by the dissolution of salts ($1\text{ m }Zn(TFSI)_2 + 20\text{ m LiTFSI}$) at extremely high concentrations in water [67]. At low concentrations of salts (e.g., $1\text{ m }Zn(TFSI)_2 + 10\text{ m LiTFSI}$), reduction occurs at low potential, resulting in H_2 evolution. At high salts concentration ($>20\text{ m}$), there is a formation of Zn^{2+} solvation sheath devoid of water molecules, and thus, the reduction potential of solvated $Zn(TFSI)_n$ increases above H_2 evolution. Additionally, at a high concentration of TFSI, the defluorination of LiTFSI take place at reduction potential greater than H_2 evolution. This transverse led to the creation of stable and effective interphase (SEI), whose existence inhibits H_2 evolution at a lower potential and allows efficient zinc plating/stripping ($CE \approx 100\%$). However, WiSE faces fundamental disadvantages such as high viscosity and high cost, and organic electrolytes are unfitting for zinc-air batteries cause of hydroxide ion non-conductivity. Therefore, either by modifying existing aqueous electrolytes, introducing a new electrolyte system, or by surface changes to the zinc anode, the development of an *in situ* Zn^{2+} -conducting SEI layer is necessary to suppress zinc anode side reactions (dendrite formation and H_2 evolution) and to improve cyclic efficiency [105,109]. Recently SEI formation in zinc-air batteries were reported by incorporating trimethylethyl ammonium trifluoromethane-sulfonate $Me_3EtN^+OTF^-$ additive in the aqueous zinc trifluoromethanesulfonate $Zn(OTF)_2$ electrolyte, which creates *in situ* fluorinated and water-repelling interphase that transfer Zn^{2+} and suppresses HER resulting in enhanced zinc plating/stripping and Coulombic efficiency of 99.9% [101]. Compared to zinc– O_2 batteries with $Zn(OTF)_2$ as sole electrolyte

(Figure 18a), the zinc–O₂ batteries with Me₃EtNOTF as additive to the Zn(OTF)₂ electrolyte display excellent performances with cycle life >300 cycles with a DoD of 68% (Figure 18b). The exceptionally reversible zinc plating/stripping chemistry with Me₃EtNOTF in the electrolyte, enables recovery of smooth zinc anode surfaces even after long-term cycling, literally decreasing the voltage hysteresis in zinc–O₂ batteries and suppressing H₂ evolution potential in contrast to Zn(OTF)₂ electrolyte. Additionally, Me₃EtNOTF addition improves the reversibility of the two-electron reaction at air cathodes. Figure 18c display a TEM image of a 64 nm thick ZnF₂ SEI developed on Zn anode after 50 cycles in Zn(OTF)₂ + Me₃EtNOTF electrolyte. The SEI was confirmed to be ZnF₂ rich; however, a detailed XPS analysis suggest also few other components such as ZnSO₃, ZnCO₃, and polyanions (Figure 18d). The ZnF₂-abundant interphase permits Zn²⁺ diffusion while protecting the zinc anode surface from water and averting parasitic side reactions.

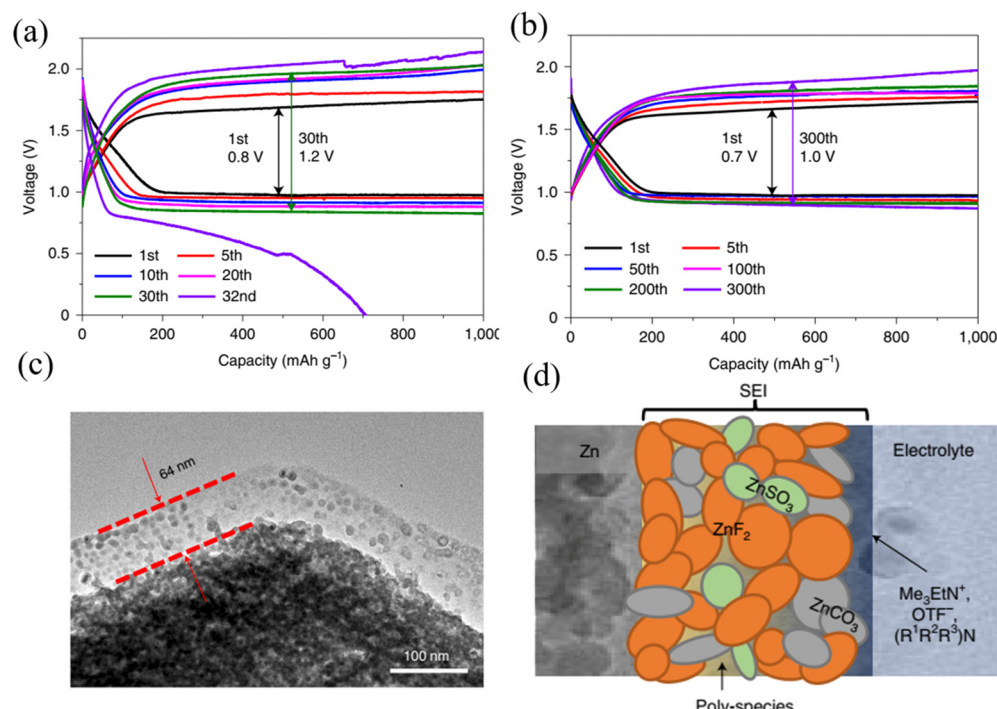


Figure 18. Cyclization profile of the zinc–O₂ batteries in the presence 4 m Zn(OTF)₂ (a) and 4 m Zn(OTF)₂ + 0.5 m Me₃EtNOTF (b) chosen cycle number at 50 mA/g and below 1000 mA h/g (cathode areal capacity equals to 0.7 mAh/cm²). TEM image of the zinc anode surface cycled in 4 m Zn(OTF)₂ + 0.5 m Me₃EtNOTF (c), the red lines mark the width of the interphase. (d) Schematic of proposed Zn²⁺-conducting SEI, realized by small nodular entities dispersed in a polymeric skeleton [101]. Reprinted with permission from Ref. [101], Copyright 2021, Springer Nature.

The tendency of a zinc anode to form non-uniform and nonplanar zinc deposits during continuous stripping/plating is one of the principal reasons of the short lifespan of rechargeable zinc–air batteries and this has drawn the focus on approaches leading to a more uniform growth of zinc during cyclization. Texturing zinc anode surface is a newly introduced effective way to improve zinc plating/stripping. It is reported that [002] a textured zinc surface is worthwhile for zinc anode reversibility [110]. Additionally, epitaxial electrodeposition of zinc with [002]-guided improves zinc reversibility remarkably [111]. For instance, ZnSO₄ electrolyte enriched with H₃PO₄ assures the [002] epitaxial development on the [002]-textured zinc surface, exhibiting reversible zinc chemistry supporting extended cyclability (Figure 19a) [38]. The H₃PO₄ act as texturing agent and initiate [002]-epitaxial growths on the textured zinc surface. Additionally, the H₃PO₄ additive incorporation helps in the creation of Zn²⁺-conducting SEI composed of zinc phosphate (140 nm, shown with arrows in SEM image Figure 19b), which further enhance the reversibility of the zinc anode.

The prepared zinc–O₂ cell displayed a cycle life of 250 h at a current density 0.1 mA/cm² with low DoD (~1%) and 50 h at a current density 1.1 mA/cm² with 20% DoD of the zinc anode as shown in Figure 19c,d. At the current density of 0.1 mA/cm² after 66 cycles, the voltage hysteresis remains unvarying, demonstrating the excellent reversibility. By replacing the electrolyte (indicated with arrow in Figure 19c), the Zn–O₂ battery displays a notable lifetime of more than 250 h. Thus, H₃PO₄ acts as an effective texturing agent which might enable aqueous zinc–air batteries competitive for the practical applications. Even though the approach mentioned above is practical to impede dendrite growth, the long-run zinc [002]-textured growths still come across challenges. For short cyclic duration [002]-textured zinc anode supports lateral growth of zinc. However, at higher DoD or long cycle time, zinc exhibit non-uniform deposition, leading to zinc dendrite generation. Thus to maintain continuous anchored [002]-textured zinc growths, a noble approach of modification of the separator was reported in a recent article [112]. A Janus separator was fabricated by growing aligned graphene treated with sulfonic cellulose on a single side of the standard glass fiber separator via a spin-coating process. The administered sulfonic cellulose provides ionic selectivity to the separator, adhering H⁺ and resisting SO₄²⁻ (ions from ZnSO₄ cell electrolyte) and thus allowing only Zn²⁺ to transport and deposit. In contrast to non-uniform deposition in the case of a standard glass fiber separator, the Janus separator leads to well-defined [002] oriented zinc growth on the zinc anode surface. The ionic selectivity and directed-growth mechanism of the Janus separator provide superior reversibility and long-term cycling durability for zinc-ion battery (Zn/MnO₂ cells), with (002)-textured deposits of zinc anode.

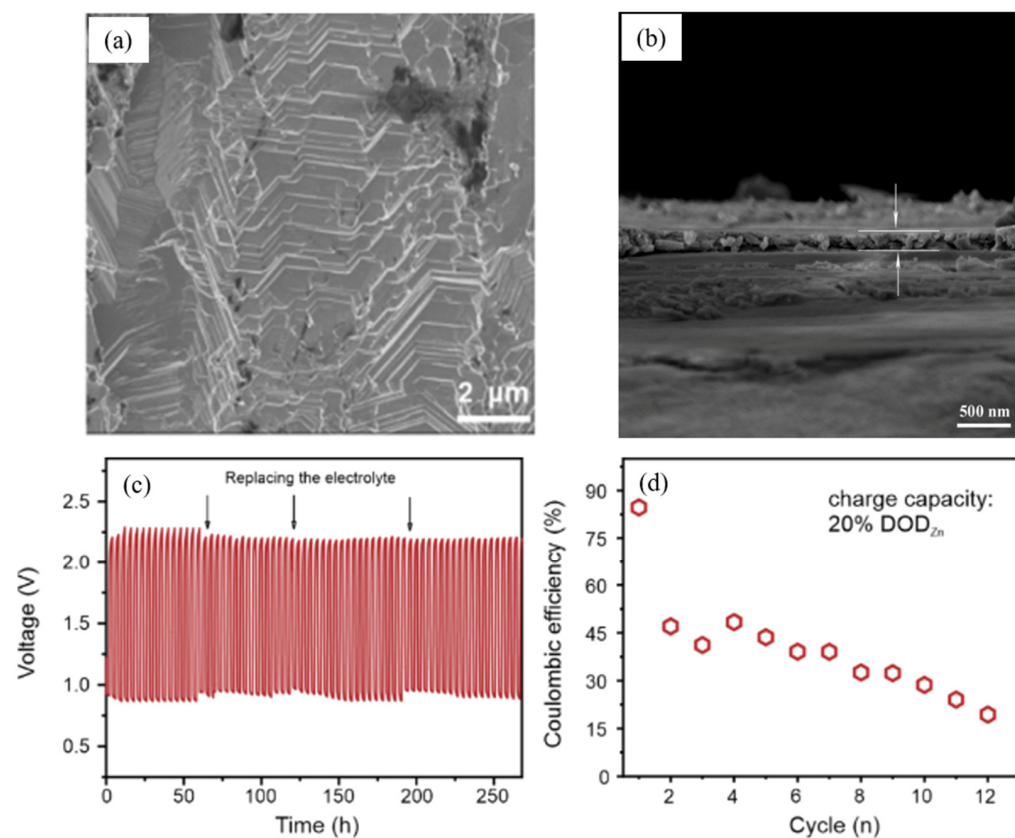


Figure 19. (a) A low-magnification SEM image of the [002]-textured zinc foil, (b) Cross-sectional SEM image of the cycled zinc showing 140 nm SEI of zinc phosphate (c) Cyclization profile of the zinc–O₂ cell (current density of 0.1 mA/cm²), (d) Coulombic efficiency of the zinc–O₂ cell with the constant charge capacity of 6 mAh/cm² (20% DoD_{Zn}) at a current density of 1.1 mA/cm², [38]. Reprinted with permission from Ref. [38], Copyright 2022, Elsevier.

The importance of SEI formation for efficient zinc–air battery operation was also observed in a solid state zinc–air battery prepared in a pouch cell architecture (ZPC) [83]. Figure 20 displayed comparison of zinc anode interaction with liquid and solid-state electrolytes. Conventional zinc anode in aqueous alkaline electrolyte promotes side reactions and zinc dendrite formation (Figure 20a,b). The ZPCs were designed with a symmetrical configuration, the cathode is three-dimensional sponge copper phosphosulfide and the electrolyte are chitosan-biocellulosics (CBCs) placed on the two sides of a patterned zinc anode (Figure 20c). The cell design assists in forming a durable SEI built on the synergic arrangement among electrostatic interactions of positively charged zinc ions and negatively charged organic entities alongside the CBC skeleton (Figure 20d). The SEI composed of Zn–S and Zn–F (<5 at%) assists in suppressing zinc passivation and exhibiting superior Coulombic efficiency. The functioning of ZPCs is administered by the ZnF/ZnS-integrated SEI embedded between CBC conductors and patterned zinc anodes. The density functional theory (DFT) simulations further disclose the bond interactions between zinc, fluorine, and sulfur atoms and their unequal charge dissemination at the interphase layer. The unequal charge scattering ($\Delta q = 1.40$ and 0.60 for Zn–S and Zn–F, respectively) expedite Zn^{2+} diffusion leading to the creation of a durable SEI, which enhance mechanical stability and shielding from the corrosion of the zinc anode.

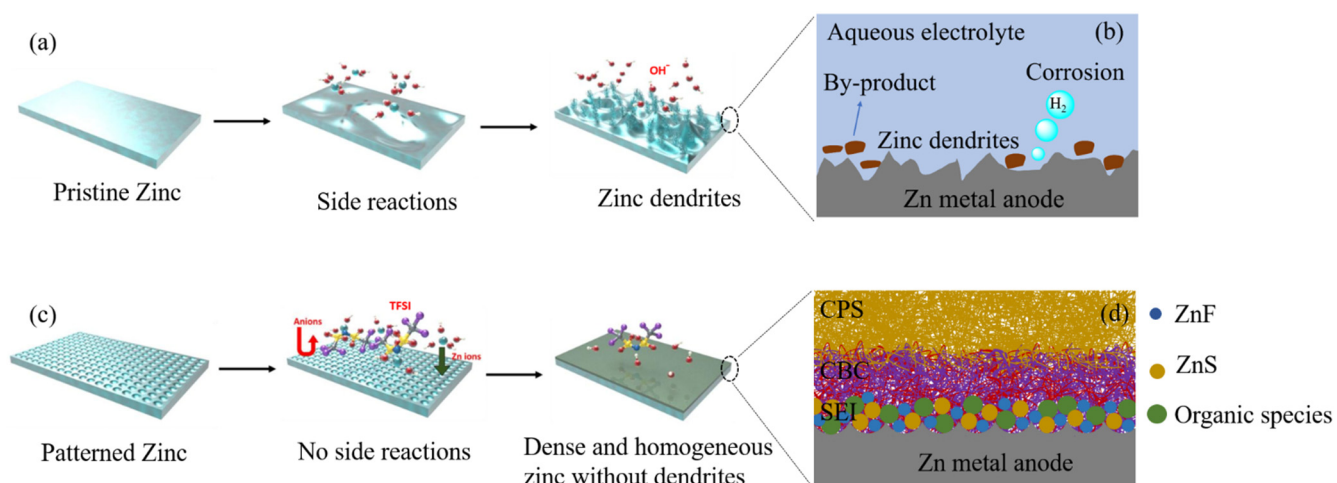


Figure 20. Schematic representation of the zinc anode interaction with liquid and solid-state electrolytes. (a,b) Conventional zinc anode in aqueous alkaline electrolyte (6 M KOH) promote the side reactions and zinc dendrites formation. (c,d) In contrast, the patterned zinc anode with CBCs solid-state electrolyte form a robust and uniform SEI layer lacking any side reactions [83]. Schematic figure (b) and (d) depicts illustration of interfacial region and SEI formation, respectively. Reprinted with permission from Ref. [83], Copyright 2021, Springer Nature.

A few reports claim that oxide surface coatings such as bismuth oxide (Bi_2O_3), indium oxide (In_2O_3), and aluminum oxide (Al_2O_3) on the surface of the zinc anode could also act as SEI [113]. For example, a sol-gel derived Al_2O_3 layer coated over a zinc anode inhibits strong interaction between active anode surface and electrolyte, leading to suppression in corrosion and self-discharge in the fabricated flexible zinc–air battery [41,114]. However, most of these coatings are ex situ physically fabricated, which are more vulnerable to detaching or cracking from the zinc anode surface because of continuous zinc volume variation during long stripping/plating cyclization. Moreover, the ex situ coatings deficit a self-repairable characteristic of in situ formed SEI, which would lose the protective function. Such ex situ coatings due to their diminished contact behavior appear less suited compared to an in situ formed SEI which are in intimate contact with the metallic anode.

2.4. Cell Design for Secondary Zinc–Air Batteries

A widely accepted and realistic laboratory test setup is required to evaluate novel materials in zinc–air battery research. Use of a standard cell design and similar experimental conditions will allow the researchers to obtain evaluation of their results, reduce the cause of irregularity and thus improve the repeatability and reliability of the obtained results. Based on the already reported cell designs, the zinc–air battery investigations are categorized into three distinct cell designs which are currently in use: beaker cells, stack cells, and coin cells. Beaker cells have an ample volume of electrolyte and comparatively small electrodes [40]. In this section we will discuss the merits and demerits of “stack cell” and “coin cell-type”, the two most widely used cell setups. Stack cell setups have planar configuration (horizontal/vertical) and were widely used for novel materials studies in a typical zinc–air battery set up. Figure 21a represents a schematic illustration of a stack cell [115]. The setup consists of two interconnected compartments, including zinc foil or a zinc plate as the anode, liquid electrolyte, and the catalyst loaded gas diffusion layer (GDL) as the air electrode/cathode. The operative area of metal anode or the air electrode is usually between 1 to 4 cm² [6,116]. The zinc–air batteries with stack cell configuration claim to deliver uniform current allocation in the zinc anode and facile O₂ evolution from the open-air cathode [2]. However, there are two problematic issues associated with stack cell zinc–air battery configuration; the use of significantly excess zinc and the open-air cathode. The excess zinc is to manage the supply during its utilization by side reactions, and this leads to considerable unused of its theoretical capacity and diminished energy density [68]. Thus, highest energy density can be attained by decreasing the weight/volume of each constituent, of which excess zinc metal anode represents a significant fragment. The disadvantage of an open-air cathode is that it accelerates electrolyte evaporation leading to loss of ion mobility and ultimately short cycle life [9].

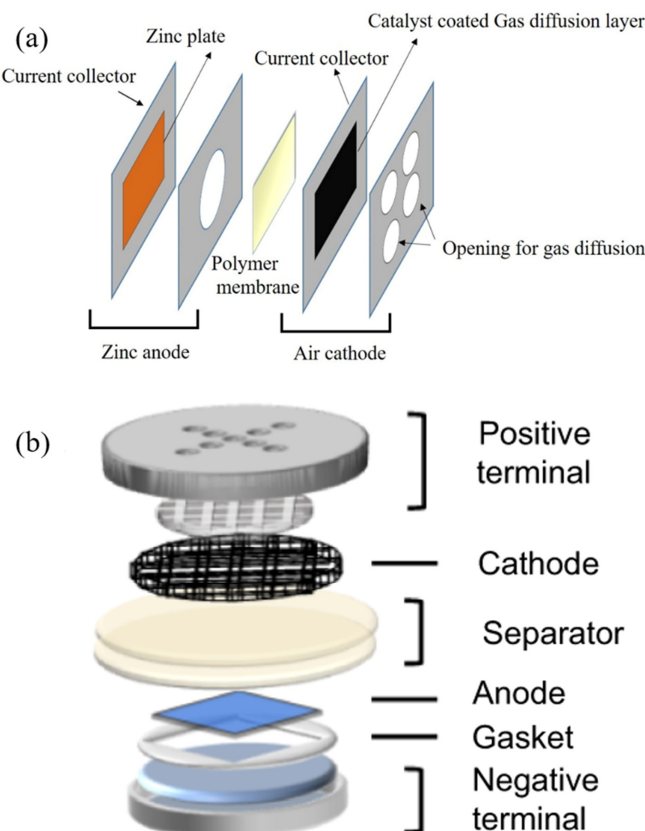


Figure 21. (a) Graphic representation of zinc–air battery stack cell configuration. Reprinted with permission from [115]; Copyright 2016, John Wiley and Sons. (b) Schematic illustration of the coin cell assembly of the zinc–air battery. Reprinted with permission from Ref. [30] Copyright 2022, Springer Nature.

Coin cell-type architectures need a minimal quantity of material and can be easily fabricated in large numbers, and because of small size, several cells can be tested simultaneously to offer good statistics for the interpretation of cell operation. Since coin-type cells include thin electrodes, problems related to the bulk electrode can be reduced, creating coin-type cells an ideal device for testing novel active materials [117]. The coin cell type has a cylindrical shape and a steel container with a relatively small electrolyte volume. It is useful for batteries using aqueous and organic electrolytes. The coin cell design is currently a standard test cell to explore new materials and electrolytes for lithium-ion batteries. Primary cells of zinc-air batteries are built in coin cell design and are available commercially for small electronic device applications. However, very few studies on rechargeable zinc-air batteries with coin cell type design are reported so far, some of which have been discussed herein [30,48,54,91]. A coin cell design is suitable for zinc-air batteries with all its basic components and its picture is shown in Figure 21b in detail [30]. Since it is easily feasible to control experimental conditions in coin cell type design and allow possible comparison and interpretation of results to already established lithium-ion batteries, a coin cell setup with a standardized designed protocol is probably the most desirable one [40,91,117,118].

3. Conclusions and Future Perspectives

This mini-review presents a brief discussion on the progress concerning the rechargeability in zinc-air batteries within the last five years. Considerable advancements have been achieved in developing rechargeable zinc-air batteries. Rechargeability needs a highly reversible process of converting the zinc anode into zinc oxide and vice versa which needs a high proportion of active material, efficient recharging, and a high capacity that could support many full charge/discharge cycles under high DoD conditions. Zinc anode structural optimization through alloying and electrodeposition was demonstrated to be effective measures for achieving the three requirements. Modifying zinc anodes, such as 3D structuring, has effectively alleviated unfavorable water-related side reactions and promoted zinc utilization due to the high inter-particle conductivity of the monolithic 3D structure electrode. At the same time, using PGEs, quasi-neutral, ionic liquids, and other alternative electrolytes assisted in facilitating water retention, reducing carbonate formation, and increasing the cycle life of the zinc-air batteries. The recently introduced novel cellulose-based SSE are promising because of their high natural abundance, low price, and renewability. Cellulose and hydrogel electrolytes-based flexible zinc-air batteries exhibit extreme temperature (-30 to 80 °C) operation due to their anti-freezing capability at low temperatures and decent water retention ability at higher temperatures. Forming durable and self-susceptible SEI is essential for enhancing anode reversibility and zinc-air battery rechargeability. In zinc-air batteries, texturing the zinc anode and adding specific additives to aqueous and solid-state electrolytes report the formation of durable zinc-ion conducting SEI. A standard cell design is required for the comparative evaluation of different research studies and should also be comparable to practical applications. Coin cell-type architectures with a minimal quantity of electrode materials and electrolytes (aqueous or organic) are suitable for zinc-air battery studies in different working conditions and can be practically used. However, the current progress of zinc-air batteries is still unsatisfactory in terms of cycle life and energy efficiencies with deep discharge and charge in contrast to conventional Li-ion batteries. Crucial obstacles remain, for instance, passivation and corrosion of zinc anode leading to low zinc utilization compared to theoretical prediction and the unresolved reaction mechanisms in quasi-neutral electrolytes, the poor ionic conductivity of PGEs in solid-state batteries, and the high price of ionic liquids. The absence of standard cell configuration and methods for evaluating the functioning of zinc-air batteries. The lack of developed computational models to evaluate experimental results and limited combined improvement techniques in a solo investigation. Hence, aside from focusing on representing results on anode design, electrode additives, and cycle lifespan, hereafter, research work need to be centered in the subsequent directions:

1. Future theoretical investigations could be helpful to provide a framework for comprehension and interpretation of experimental outcome from modified zinc anode, additives and different electrolytes. Implementing simulation results in configuration processes will help researchers crafting rechargeable zinc–air batteries with maximum zinc utilization. Implementation of advance *in situ/operando* techniques to interpret passivation and corrosion mechanism of the zinc anode under different electrolytes will help to choose best configuration with maximum zinc utilization. Future research investigation requires to focus on multiple anode problems at one time. Along experimental investigations the aim should be to consider the detrimental processes including zinc anode passivation, HER and dendritic growth altogether in the charging/discharging of the batteries. These three issues of zinc anode are correlated to each other in real applications.
2. Electrolytes portray a significant part in rechargeable zinc–air batteries and are responsible for ionic conductivity between the electrodes. In order to improve anode reversibility, researchers have supplemented traditional alkaline electrolytes with additives and polymer gel electrolytes. However, alkaline electrolytes are susceptible to atmospheric CO₂, leading to carbonate production and cell degradation. Thus, we strongly encourage more research contributions on new electrolyte systems. For instance, quasi-neutral electrolytes could completely evade the alkaline-based parasitic side reactions restricting the long-term rechargeability in zinc–air batteries. The research on quasi-neutral electrolytes is still growing slowly with only few available publications, and their specific utilization in zinc–air batteries with detailed studies is still scarce. For further advancement, it is significant to develop a thorough understanding of the anode reversibility mechanism and oxygen redox chemistries in the quasi-neutral electrolytes. The quasi-neutral electrolytes with additives such as negatively charged organic moieties facilitate solid electrostatic interaction at the electrolyte anode interface and promote SEI formation, positively affecting anode utilization and rechargeability in zinc–air batteries. Thus, robust SEI formation should be in the criteria before designing an electrolyte system for the zinc–air batteries. Flexible solid-state zinc–air batteries have appeared as another encouraging prospect in the energy field due to parallel growth in interest in portable and wearable electronic appliances. However, the practical application of flexible zinc–air batteries is inhibited due to their poor electrochemical performance and short lifespan. To deal with those issues, the core of flexible zinc–air batteries development lies in designing SSEs with flexibility, mechanical robustness, high ion conductivity, and good water retention.
3. The importance of SEI formation and its functionality in the betterment of battery performance is established for lithium-ion batteries. Because of its high redox potential, zinc is stable in both aqueous and organic electrolytes. In aqueous alkaline electrolytes, products are ionically non-conducting, which means the spontaneous generation of the SEI in zinc metal batteries is insignificant compared to the lithium-ion case. There are countable reports of SEI formation in zinc–air batteries due to additive addition in electrolytes of zinc anode structural variation. Patterning of anode surface along with addition of organic additives could lead to electrostatic interaction and development of robust and uniform SEI. Creation of robust and uniform SEI across zinc anode will lead, to uniform zinc stripping/plating, which leads to enhance reversibility of zinc anode ultimately enhancing rechargeability and cycle life of the batteries. However, an in-depth study of SEI in the zinc–air battery is still scarce, and composition of the SEI, their structure on the zinc anode and its effect on stripping/platting efficiency must be still an active research area.
4. Descriptor and cell design. To analyze the performance of zinc–air batteries, essential descriptors and metrics should be included in research reports. Discussing these significant descriptors in future research studies would assist in evaluating the practical relevancy of zinc anodes for zinc–air battery applications and permit credible cross-comparison of different research investigations. This is significant for the speedy

transport of zinc–air battery technical knowledge from mostly lab-based research towards practical applications. The anode issues arising from battery configuration design or other physical components must be addressed. Currently only a few studies take account of experimental conditions and design of battery configurations. Only a minority of research reports consider the design of battery configurations with the optimization of anodes or electrolytes to get close to commercial batteries. We suggest employing coin cell-type designs because of their near-to-commercial configuration. Standard cell designs and experimental conditions enable easy comparison and interpretation of results.

Author Contributions: S.K.Y.: Conceptualization, writing, original draft preparation, writing, review and editing, visualization; D.D.: review and editing; J.J.S.: Conceptualization, writing, review and editing, visualization, project administration, funding acquisition. All authors have read and agreed to the published version of the manuscript.

Funding: Internal funding through TUDa is acknowledged with gratitude.

Institutional Review Board Statement: Not applicable.

Informed Consent Statement: Not applicable.

Data Availability Statement: Not applicable.

Conflicts of Interest: The authors declare no conflict of interest.

References

- Li, L.; Chang, Z.; Zhang, X.-B. Recent Progress on the Development of Metal-Air Batteries. *Adv. Sustain. Syst.* **2017**, *1*, 1700036. [[CrossRef](#)]
- Fu, J.; Cano, Z.P.; Park, M.G.; Yu, A.; Fowler, M.; Chen, Z. Electrically Rechargeable Zinc–Air Batteries: Progress, Challenges, and Perspectives. *Adv. Mater.* **2017**, *29*, 1604685. [[CrossRef](#)]
- Parker, J.F.; Nelson, E.S.; Wattendorf, M.D.; Chervin, C.N.; Long, J.W.; Rolison, D.R. Retaining the 3D Framework of Zinc Sponge Anodes upon Deep Discharge in Zn-Air Cells. *ACS Appl. Mater. Interfaces* **2014**, *6*, 19471–19476. [[CrossRef](#)]
- Zhou, Z.; Zhang, Y.; Chen, P.; Wu, Y.; Yang, H.; Ding, H.; Zhang, Y.; Wang, Z.; Du, X.; Liu, N. Graphene Oxide-Modified Zinc Anode for Rechargeable Aqueous Batteries. *Chem. Eng. Sci.* **2019**, *194*, 142–147. [[CrossRef](#)]
- Zhou, T.; Zhang, N.; Wu, C.; Xie, Y. Surface/Interface Nanoengineering for Rechargeable Zn-Air Batteries. *Energy Environ. Sci.* **2020**, *13*, 1132–1153. [[CrossRef](#)]
- Olabi, A.G.; Sayed, E.T.; Wilberforce, T.; Jamal, A.; Alami, A.H.; Elsaid, K.; Mohammod, S.; Rahman, A.; Shah, S.K. Metal-Air Batteries—A Review. *Energies* **2021**, *14*, 7373. [[CrossRef](#)]
- Ren, S.; Duan, X.; Liang, S.; Zhang, M.; Zheng, H. Bifunctional Electrocatalysts for Zn-Air Batteries: Recent Developments and Future Perspectives. *J. Mater. Chem. A* **2020**, *8*, 6144–6182. [[CrossRef](#)]
- Wang, H.F.; Xu, Q. Materials Design for Rechargeable Metal-Air Batteries. *Mater.* **2019**, *1*, 565–595. [[CrossRef](#)]
- Xu, M.; Ivey, D.G.; Xie, Z.; Qu, W. Rechargeable Zn-Air Batteries: Progress in Electrolyte Development and Cell Configuration Advancement. *J. Power Sources* **2015**, *283*, 358–371. [[CrossRef](#)]
- Mainar, A.R.; Iruin, E.; Colmenares, L.C.; Kvasha, A.; de Meatza, I.; Bengoechea, M.; Leonet, O.; Boyano, I.; Zhang, Z.; Blazquez, J.A. An Overview of Progress in Electrolytes for Secondary Zinc-Air Batteries and Other Storage Systems Based on Zinc. *J. Energy Storage* **2018**, *15*, 304–328. [[CrossRef](#)]
- Prakoso, B.; Mahbub, M.A.A.; Yilmaz, M.; Khoiruddin; Wenten, I.G.; Handoko, A.D.; Sumboja, A. Recent Progress in Extending the Cycle-Life of Secondary Zn-Air Batteries. *ChemNanoMat* **2021**, *7*, 354–367. [[CrossRef](#)]
- Meng, F.L.; Liu, K.H.; Zhang, Y.; Shi, M.M.; Zhang, X.B.; Yan, J.M.; Jiang, Q. Recent Advances toward the Rational Design of Efficient Bifunctional Air Electrodes for Rechargeable Zn–Air Batteries. *Small* **2018**, *14*, 1703843. [[CrossRef](#)]
- Pan, J.; Tian, X.L.; Zaman, S.; Dong, Z.; Liu, H.; Park, H.S.; Xia, B.Y. Recent Progress on Transition Metal Oxides as Bifunctional Catalysts for Lithium-Air and Zinc-Air Batteries. *Batter. Supercaps* **2019**, *2*, 336–347. [[CrossRef](#)]
- Wang, X.; Peng, L.; Xu, N.; Wu, M.; Wang, Y.; Guo, J.; Sun, S.; Qiao, J. Cu/S-Occupation Bifunctional Oxygen Catalysts for Advanced Rechargeable Zinc-Air Batteries. *ACS Appl. Mater. Interfaces* **2020**, *12*, 52836–52844. [[CrossRef](#)]
- Zhou, C.; Chen, X.; Liu, S.; Han, Y.; Meng, H.; Jiang, Q.; Zhao, S.; Wei, F.; Sun, J.; Tan, T.; et al. Superdurable Bifunctional Oxygen Electrocatalyst for High-Performance Zinc-Air Batteries. *J. Am. Chem. Soc.* **2022**, *144*, 2694–2704. [[CrossRef](#)]
- Zhang, J.; Zhou, Q.; Tang, Y.; Zhang, L.; Li, Y. Zinc-Air Batteries: Are They Ready for Prime Time? *Chem. Sci.* **2019**, *10*, 8924–8929. [[CrossRef](#)]
- Deckenbach, D.; Schneider, J.J. A 3D Hierarchically Porous Nanoscale ZnO Anode for High-Energy Rechargeable Zinc-Air Batteries. *J. Power Sources* **2021**, *488*, 229393. [[CrossRef](#)]

18. Mainar, A.R.; Leonet, O.; Bengoechea, M.; Boyano, I.; Meatza, I.D.; Kvasha, A.; Guerfi, A.; Blázquez, J.A. Alkaline Aqueous Electrolytes for Secondary Zinc–Air Batteries: An Overview. *Int. J. Energy Res.* **2016**, *40*, 1032–1049. [[CrossRef](#)]
19. Pourzolfaghar, H.; Hosseini, S.; Zuki, F.M.; Alinejad, M.; Li, Y.Y. Recent Advancements to Mitigate Zinc Oxide Formation in Zinc–Air Batteries: A Technical Review. *Mater. Today Commun.* **2021**, *29*, 102954. [[CrossRef](#)]
20. Arise, I.; Kawai, S.; Fukunaka, Y.; McLarnon, F.R. Numerical Calculation of Ionic Mass-Transfer Rates Accompanying Anodic Zinc Dissolution in Alkaline Solution. *J. Electrochem. Soc.* **2010**, *157*, A171–A178. [[CrossRef](#)]
21. Horn, Q.C.; Shao-Horn, Y. Morphology and Spatial Distribution of ZnO Formed in Discharged Alkaline Zn/MnO₂ AA Cells. *J. Electrochem. Soc.* **2003**, *150*, A652–A658. [[CrossRef](#)]
22. Huot, J.Y.; Malservisi, M. High-Rate Capability of Zinc Anodes in Alkaline Primary Cells. *J. Power Sources* **2001**, *96*, 133–139. [[CrossRef](#)]
23. Christensen, M.K.; Mathiesen, J.K.; Simonsen, S.B.; Norby, P. Transformation and Migration in Secondary Zinc–Air Batteries Studied by: In Situ Synchrotron X-Ray Diffraction and X-Ray Tomography. *J. Mater. Chem. A* **2019**, *7*, 6459–6466. [[CrossRef](#)]
24. Mainar, A.R.; Colmenares, L.C.; Blázquez, J.A.; Urdampilleta, I. A Brief Overview of Secondary Zinc Anode Development: The Key of Improving Zinc-Based Energy Storage Systems. *Int. J. Energy Res.* **2018**, *42*, 903–918. [[CrossRef](#)]
25. Zhao, Z.; Fan, X.; Ding, J.; Hu, W.; Zhong, C.; Lu, J. Challenges in Zinc Electrodes for Alkaline Zinc–Air Batteries: Obstacles to Commercialization. *ACS Energy Lett.* **2019**, *4*, 2259–2270. [[CrossRef](#)]
26. Yu, J.; Chen, F.; Tang, Q.; Gebremariam, T.T.; Wang, J.; Gong, X.; Wang, X. Ag-Modified Cu Foams as Three-Dimensional Anodes for Rechargeable Zinc–Air Batteries. *ACS Appl. Nano Mater.* **2019**, *2*, 2679–2688. [[CrossRef](#)]
27. Li, Y.; Lu, J. Metal–Air Batteries: Will They Be the Future Electrochemical Energy Storage Device of Choice? *ACS Energy Lett.* **2017**, *2*, 1370–1377. [[CrossRef](#)]
28. Pan, Z.; Yang, J.; Zang, W.; Kou, Z.; Wang, C.; Ding, X.; Guan, C.; Xiong, T.; Chen, H.; Zhang, Q.; et al. All-Solid-State Sponge-like Squeezable Zinc–Air Battery. *Energy Storage Mater.* **2019**, *23*, 375–382. [[CrossRef](#)]
29. Parker, J.F.; Chervin, C.N.; Nelson, E.S.; Rolison, D.R.; Long, J.W. Wiring Zinc in Three Dimensions Re-Writes Battery Performance—Dendrite-Free Cycling. *Energy Environ. Sci.* **2014**, *7*, 1117–1124. [[CrossRef](#)]
30. Li, L.; Tsang, Y.C.A.; Xiao, D.; Zhu, G.; Zhi, C.; Chen, Q. Phase-Transition Tailored Nanoporous Zinc Metal Electrodes for Rechargeable Alkaline Zinc–Nickel Oxide Hydroxide and Zinc–Air Batteries. *Nat. Commun.* **2022**, *13*, 2870. [[CrossRef](#)]
31. Tian, H.; Li, Z.; Feng, G.; Yang, Z.; Fox, D.; Wang, M.; Zhou, H.; Zhai, L.; Kushima, A.; Du, Y.; et al. Stable, High-Performance, Dendrite-Free, Seawater-Based Aqueous Batteries. *Nat. Commun.* **2021**, *12*, 237. [[CrossRef](#)]
32. Peng, Y.; Lai, C.; Zhang, M.; Liu, X.; Yin, Y.; Li, Y.; Wu, Z. Zn–Sn Alloy Anode with Repressible Dendrite Grown and Meliorative Corrosion Resistance for Zn–Air Battery. *J. Power Sources* **2022**, *526*, 231173. [[CrossRef](#)]
33. Durmus, Y.E.; Montiel Guerrero, S.S.; Tempel, H.; Hausen, F.; Kunigl, H.; Eichel, R.A. Influence of Al Alloying on the Electrochemical Behavior of Zn Electrodes for Zn–Air Batteries With Neutral Sodium Chloride Electrolyte. *Front. Chem.* **2019**, *7*, 800. [[CrossRef](#)]
34. Park, D.J.; Aremu, E.O.; Ryu, K.S. Bismuth Oxide as an Excellent Anode Additive for Inhibiting Dendrite Formation in Zinc–Air Secondary Batteries. *Appl. Surf. Sci.* **2018**, *456*, 507–514. [[CrossRef](#)]
35. Jo, Y.N.; Prasanna, K.; Kang, S.H.; Ilango, P.R.; Kim, H.S.; Eom, S.W.; Lee, C.W. The Effects of Mechanical Alloying on the Self-Discharge and Corrosion Behavior in Zn–Air Batteries. *J. Ind. Eng. Chem.* **2017**, *53*, 247–252. [[CrossRef](#)]
36. Aremu, E.O.; Park, D.J.; Ryu, K.S. The Effects of Anode Additives towards Suppressing Dendrite Growth and Hydrogen Gas Evolution Reaction in Zn–Air Secondary Batteries. *Ionics* **2019**, *25*, 4197–4207. [[CrossRef](#)]
37. Chotipanich, J.; Arpornwichanop, A.; Yonezawa, T.; Kheawhom, S. Electronic and Ionic Conductivities Enhancement of Zinc Anode for Flexible Printed Zinc–Air Battery. *Eng. J.* **2018**, *22*, 47–57. [[CrossRef](#)]
38. Liu, Y.; Hu, J.; Lu, Q.; Hantusch, M.; Zhang, H.; Qu, Z.; Tang, H.; Dong, H.; Schmidt, O.G.; Holze, R.; et al. Highly Enhanced Reversibility of a Zn Anode by In-Situ Texturing. *Energy Storage Mater.* **2022**, *47*, 98–104. [[CrossRef](#)]
39. Schmid, M.; Willert-Porada, M. Electrochemical Behavior of Zinc Particles with Silica Based Coatings as Anode Material for Zinc Air Batteries with Improved Discharge Capacity. *J. Power Sources* **2017**, *351*, 115–122. [[CrossRef](#)]
40. Stock, D.; Dongmo, S.; Janek, J.; Schröder, D. Benchmarking Anode Concepts: The Future of Electrically Rechargeable Zinc–Air Batteries. *ACS Energy Lett.* **2019**, *4*, 1287–1300. [[CrossRef](#)]
41. Lee, S.M.; Kim, Y.J.; Eom, S.W.; Choi, N.S.; Kim, K.W.; Cho, S.B. Improvement in Self-Discharge of Zn Anode by Applying Surface Modification for Zn–Air Batteries with High Energy Density. *J. Power Sources* **2013**, *227*, 177–184. [[CrossRef](#)]
42. Sun, W.; Ma, M.; Zhu, M.; Xu, K.; Xu, T.; Zhu, Y.; Qian, Y. Chemical Buffer Layer Enabled Highly Reversible Zn Anode for Deeply Discharging and Long-Life Zn–Air Battery. *Small* **2022**, *18*, 2106604. [[CrossRef](#)]
43. Zhang, Y.; Wu, Y.; Ding, H.; Yan, Y.; Zhou, Z.; Ding, Y.; Liu, N. Sealing ZnO Nanorods for Deeply Rechargeable High-Energy Aqueous Battery Anodes. *Nano Energy* **2018**, *53*, 666–674. [[CrossRef](#)]
44. Zhang, Y.; Wu, Y.; You, W.; Tian, M.; Huang, P.W.; Zhang, Y.; Sun, Z.; Ma, Y.; Hao, T.; Liu, N. Deeply Rechargeable and Hydrogen-Evolution-Suppressing Zinc Anode in Alkaline Aqueous Electrolyte. *Nano Lett.* **2020**, *20*, 4700–4707. [[CrossRef](#)]
45. Kim, Y.J.; Ryu, K.S. The Surface-Modified Effects of Zn Anode with CuO in Zn–Air Batteries. *Appl. Surf. Sci.* **2019**, *480*, 912–922. [[CrossRef](#)]
46. Wu, Y.; Zhang, Y.; Ma, Y.; Howe, J.D.; Yang, H.; Chen, P.; Aluri, S.; Liu, N. Ion-Sieving Carbon Nanoshells for Deeply Rechargeable Zn-Based Aqueous Batteries. *Adv. Energy Mater.* **2018**, *8*, 1802470. [[CrossRef](#)]

47. Leong, K.W.; Wang, Y.; Ni, M.; Pan, W.; Luo, S.; Leung, D.Y.C. Rechargeable Zn-Air Batteries: Recent Trends and Future Perspectives. *Renew. Sustain. Energy Rev.* **2022**, *154*, 111771. [\[CrossRef\]](#)
48. Schmid, M.; Willert-Porada, M. Zinc Particles Coated with Bismuth Oxide Based Glasses as Anode Material for Zinc Air Batteries with Improved Electrical Rechargeability. *Electrochim. Acta* **2018**, *260*, 246–253. [\[CrossRef\]](#)
49. Nam Jo, Y.; Santhoshkumar, P.; Prasanna, K.; Vediappan, K.; Woo Lee, C. Improving Self-Discharge and Anti-Corrosion Performance of Zn-Air Batteries Using Conductive Polymer-Coated Zn Active Materials. *J. Ind. Eng. Chem.* **2019**, *76*, 396–402. [\[CrossRef\]](#)
50. Deyab, M.A.; Mele, G. Polyaniline/Zn-Phthalocyanines Nanocomposite for Protecting Zinc Electrode in Zn-Air Battery. *J. Power Sources* **2019**, *443*, 227264. [\[CrossRef\]](#)
51. Zhang, Z.; Zhou, D.; Huang, G.H.; Zhou, L.; Huang, B. Preparation and Properties of ZnO/PVA/β-CD/PEG Composite Electrode for Rechargeable Zinc Anode. *J. Electroanal. Chem.* **2018**, *827*, 85–92. [\[CrossRef\]](#)
52. Stock, D.; Dongmo, S.; Walther, F.; Sann, J.; Janek, J.; Schröder, D. Homogeneous Coating with an Anion-Exchange Ionomer Improves the Cycling Stability of Secondary Batteries with Zinc Anodes. *ACS Appl. Mater. Interfaces* **2018**, *10*, 8640–8648. [\[CrossRef\]](#) [\[PubMed\]](#)
53. Stock, D.; Dongmo, S.; Damtew, D.; Stumpp, M.; Konovalova, A.; Henkensmeier, D.; Schlettwein, D.; Schröder, D. Design Strategy for Zinc Anodes with Enhanced Utilization and Retention: Electrodeposited Zinc Oxide on Carbon Mesh Protected by Ionomeric Layers. *ACS Appl. Energy Mater.* **2018**, *1*, 5579–5588. [\[CrossRef\]](#)
54. Stock, D.; Dongmo, S.; Miyazaki, K.; Abe, T.; Janek, J.; Schröder, D. Towards Zinc-Oxygen Batteries with Enhanced Cycling Stability: The Benefit of Anion-Exchange Ionomer for Zinc Sponge Anodes. *J. Power Sources* **2018**, *395*, 195–204. [\[CrossRef\]](#)
55. Chang, J.; Wang, G.; Yang, Y. Recent Advances in Electrode Design for Rechargeable Zinc–Air Batteries. *Small Sci.* **2021**, *1*, 2100044. [\[CrossRef\]](#)
56. Parker, J.F.; Ko, J.S.; Rolison, D.R.; Long, J.W. Translating Materials-Level Performance into Device-Relevant Metrics for Zinc-Based Batteries. *Joule* **2018**, *2*, 2519–2527. [\[CrossRef\]](#)
57. Mainar, A.R.; Colmenares, L.C.; Grande, H.J.; Blázquez, J.A. Enhancing the Cycle Life of a Zinc–Air Battery by Means of Electrolyte Additives and Zinc Surface Protection. *Batteries* **2018**, *4*, 46. [\[CrossRef\]](#)
58. Tran, T.N.T.; Chung, H.; Ivey, D.G. A Study of Alkaline Gel Polymer Electrolytes for Rechargeable Zinc–Air Batteries. *Electrochim. Acta* **2019**, *327*, 135021. [\[CrossRef\]](#)
59. Liu, X.; Fan, X.; Liu, B.; Ding, J.; Deng, Y.; Han, X.; Zhong, C.; Hu, W. Mapping the Design of Electrolyte Materials for Electrically Rechargeable Zinc–Air Batteries. *Adv. Mater.* **2021**, *33*, 2006461. [\[CrossRef\]](#)
60. Schröder, D.; Sinai Borker, N.N.; König, M.; Kreuer, U. Performance of Zinc Air Batteries with Added K_2CO_3 in the Alkaline Electrolyte. *J. Appl. Electrochem.* **2015**, *45*, 427–437. [\[CrossRef\]](#)
61. Liu, S.; Han, W.; Cui, B.; Liu, X.; Zhao, F.; Stuart, J.; Licht, S. A Novel Rechargeable Zinc–Air Battery with Molten Salt Electrolyte. *J. Power Sources* **2017**, *342*, 435–441. [\[CrossRef\]](#)
62. Li, Y.; Fan, X.; Liu, X.; Qu, S.; Liu, J.; Ding, J.; Han, X.; Deng, Y.; Hu, W.; Zhong, C. Long-Battery-Life Flexible Zinc–Air Battery with near-Neutral Polymer Electrolyte and Nanoporous Integrated Air Electrode. *J. Mater. Chem. A* **2019**, *7*, 25449–25457. [\[CrossRef\]](#)
63. Xiao, C.; Yao, R.; Zhu, H.; Qian, L.; Yang, C. Choline Chloride Enhances the Electrochemical Stability of Zinc Plating/Stripping. *Chem. Commun.* **2022**, *58*, 10088–10090. [\[CrossRef\]](#) [\[PubMed\]](#)
64. Ingale, P.; Sakthivel, M.; Drillet, J.-F. Test of Diethylmethylammonium Trifluoromethanesulfonate Ionic Liquid as Electrolyte in Electrically Rechargeable Zn/Air Battery. *J. Electrochem. Soc.* **2017**, *164*, H5224–H5229. [\[CrossRef\]](#)
65. Hwang, H.J.; Chi, W.S.; Kwon, O.; Lee, J.G.; Kim, J.H.; Shul, Y.G. Selective Ion Transporting Polymerized Ionic Liquid Membrane Separator for Enhancing Cycle Stability and Durability in Secondary Zinc–Air Battery Systems. *ACS Appl. Mater. Interfaces* **2016**, *8*, 26298–26308. [\[CrossRef\]](#) [\[PubMed\]](#)
66. Fu, J.; Lee, D.U.; Hassan, F.M.; Bai, Z.; Park, M.G.; Chen, Z. Flexible High-Energy Polymer-Electrolyte-Based Rechargeable Zinc–Air Batteries. *Adv. Mater.* **2015**, *27*, 5617–5622. [\[CrossRef\]](#)
67. Wang, F.; Borodin, O.; Gao, T.; Fan, X.; Sun, W.; Han, F.; Faraone, A.; Dura, J.A.; Xu, K.; Wang, C. Highly Reversible Zinc Metal Anode for Aqueous Batteries. *Nat. Mater.* **2018**, *17*, 543–549. [\[CrossRef\]](#)
68. Sun, W.; Wang, F.; Zhang, B.; Zhang, M.; Küpers, V.; Ji, X.; Theile, C.; Bieker, P.; Xu, K.; Wang, C.; et al. A Rechargeable Zinc–Air Battery Based on Zinc Peroxide Chemistry. *Science* **2021**, *371*, 46–51. [\[CrossRef\]](#)
69. Chen, P.; Zhang, K.; Tang, D.; Liu, W.; Meng, F.; Huang, Q.; Liu, J. Recent Progress in Electrolytes for Zn–Air Batteries. *Front. Chem.* **2020**, *8*, 372. [\[CrossRef\]](#)
70. Sumboja, A.; Lübke, M.; Wang, Y.; An, T.; Zong, Y.; Liu, Z. All-Solid-State, Foldable, and Rechargeable Zn–Air Batteries Based on Manganese Oxide Grown on Graphene-Coated Carbon Cloth Air Cathode. *Adv. Energy Mater.* **2017**, *7*, 1700927. [\[CrossRef\]](#)
71. Hao, J.; Li, X.; Zeng, X.; Li, D.; Mao, J.; Guo, Z. Deeply Understanding the Zn Anode Behaviour and Corresponding Improvement Strategies in Different Aqueous Zn-Based Batteries. *Energy Environ. Sci.* **2020**, *13*, 3917–3949. [\[CrossRef\]](#)
72. Pei, Z.; Yuan, Z.; Wang, C.; Zhao, S.; Fei, J.; Wei, L.; Chen, J.; Wang, C.; Qi, R.; Liu, Z.; et al. A Flexible Rechargeable Zinc–Air Battery with Excellent Low-Temperature Adaptability. *Angew. Chem. Int. Ed.* **2020**, *59*, 4793–4799. [\[CrossRef\]](#) [\[PubMed\]](#)
73. Fan, X.; Liu, J.; Song, Z.; Han, X.; Deng, Y.; Zhong, C.; Hu, W. Porous Nanocomposite Gel Polymer Electrolyte with High Ionic Conductivity and Superior Electrolyte Retention Capability for Long-Cycle-Life Flexible Zinc–Air Batteries. *Nano Energy* **2019**, *56*, 454–462. [\[CrossRef\]](#)

74. Song, Z.; Ding, J.; Liu, B.; Liu, X.; Han, X.; Deng, Y.; Hu, W.; Zhong, C. A Rechargeable Zn–Air Battery with High Energy Efficiency and Long Life Enabled by a Highly Water-Retentive Gel Electrolyte with Reaction Modifier. *Adv. Mater.* **2020**, *32*, 1908127. [CrossRef] [PubMed]
75. Fu, J.; Zhang, J.; Song, X.; Zarrin, H.; Tian, X.; Qiao, J.; Rasen, L.; Li, K.; Chen, Z. A Flexible Solid-State Electrolyte for Wide-Scale Integration of Rechargeable Zinc–Air Batteries. *Energy Environ. Sci.* **2016**, *9*, 663–670. [CrossRef]
76. Huang, Y.; Li, Z.; Pei, Z.; Liu, Z.; Li, H.; Zhu, M.; Fan, J.; Dai, Q.; Zhang, M.; Dai, L.; et al. Solid-State Rechargeable Zn / NiCo and Zn–Air Batteries with Ultralong Lifetime and High Capacity: The Role of a Sodium Polyacrylate Hydrogel Electrolyte. *Adv. Energy Mater.* **2018**, *8*, 1802288. [CrossRef]
77. Dou, H.; Xu, M.; Zheng, Y.; Li, Z.; Wen, G.; Zhang, Z.; Yang, L.; Ma, Q.; Yu, A.; Luo, D.; et al. Bioinspired Tough Solid-State Electrolyte for Flexible Ultralong-Life Zinc–Air Battery. *Adv. Mater.* **2022**, *34*, 2110585. [CrossRef]
78. Zhang, J.; Fu, J.; Song, X.; Jiang, G.; Zarrin, H.; Xu, P.; Li, K.; Yu, A.; Chen, Z. Laminated Cross-Linked Nanocellulose/Graphene Oxide Electrolyte for Flexible Rechargeable Zinc–Air Batteries. *Adv. Energy Mater.* **2016**, *6*, 1600476. [CrossRef]
79. Zhao, N.; Wu, F.; Xing, Y.; Qu, W.; Chen, N.; Shang, Y.; Yan, M.; Li, Y.; Li, L.; Chen, R. Flexible Hydrogel Electrolyte with Superior Mechanical Properties Based on Poly(Vinyl Alcohol) and Bacterial Cellulose for the Solid-State Zinc–Air Batteries. *ACS Appl. Mater. Interfaces* **2019**, *11*, 15537–15542. [CrossRef]
80. Wei, Y.; Wang, M.; Xu, N.; Peng, L.; Mao, J.; Gong, Q.; Qiao, J. Alkaline Exchange Polymer Membrane Electrolyte for High Performance of All-Solid-State Electrochemical Devices. *ACS Appl. Mater. Interfaces* **2018**, *10*, 29593–29598. [CrossRef]
81. Wang, M.; Xu, N.; Fu, J.; Liu, Y.; Qiao, J. High-Performance Binary Cross-Linked Alkaline Anion Polymer Electrolytes for All-Solid-State Supercapacitors and Flexible Rechargeable Zinc–Air Batteries. *J. Mater. Chem. A* **2019**, *7*, 11257–11264. [CrossRef]
82. Xu, M.; Dou, H.; Zhang, Z.; Zheng, Y.; Ren, B.; Ma, Q.; Wen, G.; Luo, D.; Yu, A.; Zhang, L.; et al. Hierarchically Nanostructured Solid-State Electrolyte for Flexible Rechargeable Zinc–Air Batteries. *Angew. Chem. Int. Ed.* **2022**, *61*, e202117703. [CrossRef]
83. Shinde, S.S.; Jung, J.Y.; Wagh, N.K.; Lee, C.H.; Kim, D.H.; Kim, S.H.; Lee, S.U.; Lee, J.H. Ampere-Hour-Scale Zinc–Air Pouch Cells. *Nat. Energy* **2021**, *6*, 592–604. [CrossRef]
84. Zuo, Y.; Wang, K.; Zhao, S.; Wei, M.; Liu, X.; Zhang, P. A High Areal Capacity Solid-State Zinc–Air Battery via Interface Optimization of Electrode and Electrolyte. *Chem. Eng. J.* **2022**, *430*, 132996. [CrossRef]
85. Famprikis, T.; Canepa, P.; Dawson, J.A.; Islam, M.S.; Masquelier, C. Fundamentals of Inorganic Solid-State Electrolytes for Batteries. *Nat. Mater.* **2019**, *18*, 1278–1291. [CrossRef] [PubMed]
86. Wu, M.; Zhang, G.; Du, L.; Yang, D.; Yang, H.; Sun, S. Defect Electrocatalysts and Alkaline Electrolyte Membranes in Solid-State Zinc–Air Batteries: Recent Advances, Challenges, and Future Perspectives. *Small Methods* **2021**, *5*, 2000868. [CrossRef] [PubMed]
87. Balaish, M.; Kraytsberg, A.; Ein-Eli, Y. A Critical Review on Lithium–Air Battery Electrolytes. *Phys. Chem. Chem. Phys.* **2014**, *16*, 2801–2822. [CrossRef]
88. Simons, T.J.; Torriero, A.A.J.; Howlett, P.C.; MacFarlane, D.R.; Forsyth, M. High Current Density, Efficient Cycling of Zn^{2+} in 1-Ethyl-3-Methylimidazolium Dicyanamide Ionic Liquid: The Effect of Zn^{2+} Salt and Water Concentration. *Electrochim. Commun.* **2012**, *18*, 119–122. [CrossRef]
89. Kar, M.; Simons, T.J.; Forsyth, M.; MacFarlane, D.R. Ionic Liquid Electrolytes as a Platform for Rechargeable Metal–Air Batteries: A Perspective. *Phys. Chem. Chem. Phys.* **2014**, *16*, 18658–18674. [CrossRef]
90. Ghazvini, M.S.; Pulletikurthi, G.; Cui, T.; Kuhl, C.; Endres, F. Electrodeposition of Zinc from 1-Ethyl-3-Methylimidazolium Acetate-Water Mixtures: Investigations on the Applicability of the Electrolyte for Zn–Air Batteries. *J. Electrochem. Soc.* **2018**, *165*, D354–D363. [CrossRef]
91. Sakthivel, M.; Batchu, S.P.; Shah, A.A.; Kim, K.; Peters, W.; Drillet, J.F. An Electrically Rechargeable Zinc/Air Cell with an Aqueous Choline Acetate Electrolyte. *Materials* **2020**, *13*, 2975. [CrossRef] [PubMed]
92. Zhang, B.; Zheng, X.; Voznyy, O.; Comin, R.; Bajdich, M.; García-Melchor, M.; Han, L.; Xu, J.; Liu, M.; Zheng, L.; et al. Homogeneously Dispersed Multimetal Oxygen-Evolving Catalysts. *Science* **2016**, *352*, 333–337. [CrossRef] [PubMed]
93. An, L.; Huang, B.; Zhang, Y.; Wang, R.; Zhang, N.; Dai, T.; Xi, P.; Yan, C.H. Interfacial Defect Engineering for Improved Portable Zinc–Air Batteries with a Broad Working Temperature. *Angew. Chem. Int. Ed.* **2019**, *58*, 9459–9463. [CrossRef] [PubMed]
94. Pei, Z.; Ding, L.; Wang, C.; Meng, Q.; Yuan, Z.; Zhou, Z.; Zhao, S.; Chen, Y. Make It Stereoscopic: Interfacial Design for Full-Temperature Adaptive Flexible Zinc–Air Batteries. *Energy Environ. Sci.* **2021**, *14*, 4926–4935. [CrossRef]
95. Wang, Q.; Feng, Q.; Lei, Y.; Tang, S.; Xu, L.; Xiong, Y.; Fang, G.; Wang, Y.; Yang, P.; Liu, J.; et al. Quasi-Solid-State Zn–Air Batteries with an Atomically Dispersed Cobalt Electrocatalyst and Organohydrogel Electrolyte. *Nat. Commun.* **2022**, *13*, 3689. [CrossRef] [PubMed]
96. Chen, R.; Xu, X.; Peng, S.; Chen, J.; Yu, D.; Xiao, C.; Li, Y.; Chen, Y.; Hu, X.; Liu, M.; et al. A Flexible and Safe Aqueous Zinc–Air Battery with a Wide Operating Temperature Range from -20 to 70 °C. *ACS Sustain. Chem. Eng.* **2020**, *8*, 11501–11511. [CrossRef]
97. Zhao, C.X.; Liu, J.N.; Yao, N.; Wang, J.; Ren, D.; Chen, X.; Li, B.Q.; Zhang, Q. Can Aqueous Zinc–Air Batteries Work at Sub-Zero Temperatures? *Angew. Chem. Int. Ed.* **2021**, *60*, 15281–15285. [CrossRef]
98. Goodenough, J.B.; Park, K.S. The Li-Ion Rechargeable Battery: A Perspective. *J. Am. Chem. Soc.* **2013**, *135*, 1167–1176. [CrossRef]
99. Tripathi, A.M.; Su, W.N.; Hwang, B.J. In Situ Analytical Techniques for Battery Interface Analysis. *Chem. Soc. Rev.* **2018**, *47*, 736–751. [CrossRef]
100. Wu, F.; Yu, Y. Toward True Lithium–Air Batteries. *Joule* **2018**, *2*, 815–817. [CrossRef]

101. Cao, L.; Li, D.; Pollard, T.; Deng, T.; Zhang, B.; Yang, C.; Chen, L.; Vatamanu, J.; Hu, E.; Hourwitz, M.J.; et al. Fluorinated Interphase Enables Reversible Aqueous Zinc Battery Chemistries. *Nat. Nanotechnol.* **2021**, *16*, 902–910. [[CrossRef](#)] [[PubMed](#)]
102. Zhao, Q.; Stalin, S.; Archer, L.A. Stabilizing Metal Battery Anodes through the Design of Solid Electrolyte Interphases. *Joule* **2021**, *5*, 1119–1142. [[CrossRef](#)]
103. Popovic, J. The Importance of Electrode Interfaces and Interphases for Rechargeable Metal Batteries. *Nat. Commun.* **2021**, *12*, 8–12. [[CrossRef](#)] [[PubMed](#)]
104. Shin, J.; Lee, J.; Park, Y.; Choi, J.W. Aqueous Zinc Ion Batteries: Focus on Zinc Metal Anodes. *Chem. Sci.* **2020**, *11*, 2028–2044. [[CrossRef](#)]
105. Liang, G.; Zhi, C. A Reversible Zn-Metal Battery. *Nat. Nanotechnol.* **2021**, *16*, 853–855. [[CrossRef](#)] [[PubMed](#)]
106. Qiu, H.; Du, X.; Zhao, J.; Wang, Y.; Ju, J.; Chen, Z.; Hu, Z.; Yan, D.; Zhou, X.; Cui, G. Zinc Anode-Compatible in-Situ Solid Electrolyte Interphase via Cation Solvation Modulation. *Nat. Commun.* **2019**, *10*, 5374. [[CrossRef](#)]
107. Cao, L.; Li, D.; Deng, T.; Li, Q.; Wang, C. Hydrophobic Organic-Electrolyte-Protected Zinc Anodes for Aqueous Zinc Batteries. *Angew. Chem. Int. Ed.* **2020**, *59*, 19292–19296. [[CrossRef](#)]
108. Suo, L.; Borodin, O.; Gao, T.; Olguin, M.; Ho, J.; Fan, X.; Luo, C.; Wang, C.; Xu, K. “Water-in-Salt” Electrolyte Enables High-Voltage Aqueous Lithium-Ion Chemistries. *Science* **2015**, *350*, 938–943. [[CrossRef](#)]
109. Zheng, J.; Archer, L.A. Controlling Electrochemical Growth of Metallic Zinc Electrodes: Toward Affordable Rechargeable Energy Storage Systems. *Sci. Adv.* **2021**, *7*, eabe0219. [[CrossRef](#)]
110. Zhou, M.; Guo, S.; Li, J.; Luo, X.; Liu, Z.; Zhang, T.; Cao, X.; Long, M.; Lu, B.; Pan, A.; et al. Surface-Preferred Crystal Plane for a Stable and Reversible Zinc Anode. *Adv. Mater.* **2021**, *33*, 2100187. [[CrossRef](#)]
111. Zheng, J.; Zhao, Q.; Tang, T.; Yin, J.; Quilty, C.D.; Renderos, G.D.; Liu, X.; Deng, Y.; Wang, L.; Bock, D.C.; et al. Reversible Epitaxial Electrodeposition of Metals in Battery Anodes. *Science* **2019**, *366*, 645–648. [[CrossRef](#)] [[PubMed](#)]
112. Zhang, X.; Li, J.; Qi, K.; Yang, Y.; Liu, D.; Wang, T.; Liang, S.; Lu, B.; Zhu, Y.; Zhou, J. An Ion-Sieving Janus Separator toward Planar Electrodeposition for Deeply Rechargeable Zn-Metal Anodes. *Adv. Mater.* **2022**, *34*, 2205175. [[CrossRef](#)] [[PubMed](#)]
113. Yano, M.; Fujitani, S.; Nishio, K.; Akai, Y.; Kurimura, M. Effect of Additives in Zinc Alloy Powder on Suppressing Hydrogen Evolution. *J. Power Sources* **1998**, *74*, 129–134. [[CrossRef](#)]
114. Wongrujipairoj, K.; Poolnapol, L.; Arpornwichanop, A.; Suren, S.; Kheawhom, S. Suppression of Zinc Anode Corrosion for Printed Flexible Zinc-air Battery. *Phys. Status Solidi Basic Res.* **2017**, *254*, 1600442. [[CrossRef](#)]
115. Park, M.G.; Lee, D.U.; Seo, M.H.; Cano, Z.P.; Chen, Z. 3D Ordered Mesoporous Bifunctional Oxygen Catalyst for Electrically Rechargeable Zinc-Air Batteries. *Small* **2016**, *12*, 2707–2714. [[CrossRef](#)] [[PubMed](#)]
116. Liu, Q.; Pan, Z.; Wang, E.; An, L.; Sun, G. Aqueous Metal-Air Batteries: Fundamentals and Applications. *Energy Storage Mater.* **2020**, *27*, 478–505. [[CrossRef](#)]
117. Bonnick, P.; Dahn, J.R. A Simple Coin Cell Design for Testing Rechargeable Zinc-Air or Alkaline Battery Systems Service A Simple Coin Cell Design for Testing Rechargeable Zinc-Air. *J. Electrochem. Soc.* **2012**, *159*, A981–A989. [[CrossRef](#)]
118. Dongmo, S.; Jakob, J.; Kreissl, A.; Miyazaki, K.; Abe, T.; You, T.; Hu, C.; Schröder, D. Reproducible and Stable Cycling Performance Data on Secondary Zinc Oxygen Batteries. *Sci. Data* **2020**, *7*, 395. [[CrossRef](#)]